Passive UHF RFID tag design for mounting on cylindrical metallic surfaces

Carlos David Morales Peña

Universidade Federal de Minas Gerais
Escola de Engenharia
Programa de Pós-Graduação em Engenharia Elétrica
Belo Horizonte, Brazil
2018

Passive UHF RFID tag design for mounting on cylindrical metallic surfaces

Carlos David Morales Peña

Dissertation submitted to the Electrical Engineering Graduate Program at the Federal University of Minas Gerais, in partial fulfillment of the requirements for the degree of:
Master in Electrical Engineering

Advisor:
Prof. PhD. Diogo Batista de Oliveira

Co-Advisor:
Prof. PhD. Elson José da Silva

Universidade Federal de Minas Gerais
Escola de Engenharia
Programa de Pós-Graduação em Engenharia Elétrica
Belo Horizonte, Brazil
2018

We keep moving forward, opening new doors, and doing new things, because we're curious and curiosity keeps leading us down new paths. Then, all our dreams can come true, if we have the courage to pursue them.
Walt Disney.

Acknowledgments

I would first like to thank to God for his blessings, good health and well-being that were necessary to complete this goal.

I wish to express my sincere thanks to my family, specially my mother, for her support, advices, love, prayers and patient, I also thank my father, brother and grandparents for the unceasing encouragement and support to keep achieving my dreams. You are my motivation.

I am also grateful with the university staff: my advisors, Prof. Elson and Prof. Diogo, for the comprehension, patience, support and for all the knowledge received in order to develop my research; and Prof. Ricardo for the given support. Also, to the professors who transmitted me teachings and knowledges and the Federal University of Minas Gerais to allow me to live this amazing experience in this great country.

My sincere thanks also goes to my partners, specially to Angie, Eduard, Diego, Jose, Solival, Colombians mates and members of LEA and GAPTEM group, who supported me through this adventure. Also, to Paulo and Rafaela for teach me a little bit on the Brazilian culture and for the French lessons.

Last but not the least, to thank the CEFET and Prof. Úrsula, for allowing me to develop the antenna measurements in the laboratories; and Capes for the scholarship, which it was very important to complete my studies.

Resumo

Esta pesquisa propõe uma etiqueta passiva flexível que opera na faixa de 902-928 MHz de Ultra Alta Frequência (UHF) para aplicações de Radio Frequency Identification (RFID). A antena pequena tem uma dimensão de 13 mm x 28 mm x 0.4 mm e está composta de um substrato comercial flexível com facilidade de obtenção, para ser colada sobre superfícies cilíndricas metálicas com diferentes tamanhos.

A geometria da antena foi otimizada, usando o algoritmo genético, para maximizar sua distância de leitura. O desempenho da antena foi avaliado sobre superfícies planas e curvas, através de simulações da impedância de entrada, ganho, coeficiente de reflexão e distância de leitura. Além disso, medições do coeficiente de reflexão da etiqueta foram desenvolvidos. Os resultados da etiqueta RFID provam que a antena proposta pode ser utilizada sobre superfícies metálicas cilíndricas com uma distância de leitura superior a um metro para aplicações relacionadas com gestão de ativos industriais, controle de acesso, equipamentos médicos e da construção, identificação de peças metálicas pequenas como ferramentas, instrumentos de cozinha, recipientes metálicos e sprays.

Adicionalmente, neste trabalho foi estudado o comportamento eletromagnético da antena sobre cilindros fabricados com materiais de polyethylene terephthalate (PET) para garrafas plásticas. Baseado no processo de otimização, que tem como objetivo maximizar o raio de cobertura da etiqueta, uma distância de leitura de um metro foi conseguida. Os resultados mostram que a antena tem um comportamento confiável e útil sobre cilindros com pequeno raio. Além disso, a adição de líquidos dentro do material PET, dependendo de sua permissividade, pode incrementar a distância de leitura da etiqueta RFID.

Palabras-chave: Antena pequena, Curvatura da antena, Distância de leitura, Substrato flexível, RFID.

Abstract

This research proposes an Ultra High Frequency (UHF) flexible passive tag antenna for Radio Frequency Identification (RFID) which operates at 902-928 MHz band frequency. The small antenna has a dimension of 13 mm x 28 mm x 0.4 mm and contains a flexible commercial substrate with ease of obtaining, for being attached over flat and cylindrical metallic surfaces with different sizes.

The geometry of the tag antenna was optimized, using a genetic algorithm, maximizing its read range at 915 MHz. The antenna performance was evaluated on flat and curved surfaces, by simulations of input impedance, gain, reflection coefficient and read range. Also, measurements of reflection coefficient of the tag antenna were developed. The results of the RFID tag prove that the designed antenna can be wrapped on cylindrical metallic surfaces with read ranges above one meter, useful for applications of industrial asset management, access control, construction and medical equipment, and identification of small metallic items such as hardware tools, kitchenware, tin cans, and spray bottles.

Additionally, in this work, a study about the electromagnetic behavior of the tag antenna mounted on cylinders fabricated with polyethylene terephthalate (PET) materials was developed. Based on optimization process, whose goal is maximizing the coverage ratio of the tag antenna, a read range of about one meter is obtained. Results show that the antenna has a reliable and useful behavior over cylinders with small radius. Furthermore, the addition of a liquid component inside the PET volume, depending on its permittivity, can increase the read range of the tag antenna.

Keywords: Antenna curvature, Flexible substrate, Read range, RFID, Small antenna.

Table of Contents

Acknowledgments iv

Resumo v

Abstract vi

1 Introduction 1
1.1 Objectives . . . 5

2 Antenna Design and Methodology 6
2.1 Antenna Characteristics of the original work . . . 6
2.2 Selection of the substrate . . . 7
2.3 Characteristics of the selected tag antenna . . . 9
2.3.1 T-matching . . . 10
2.3.2 Shaped slots . . . 14
2.4 Optimization problem . . . 15
2.5 Search space of optimization . . . 17

3 Simulation results 23
3.1 Computational model . . . 23
3.2 Optimization on copper plate . . . 23
3.2.1 Antenna performance on copper plate . . . 23
3.2.2 Antenna performance on copper cylinder . . . 28
3.3 Optimization on copper cylinder . . . 34
3.4 Optimization on PET cylinder . . . 41
3.5 Discussions . . . 48

4 Measurements 50
4.1 Differential S-parameter method . . . 50
4.2 Test fixture . . . 52
4.3 Measurement process . . . 53
4.4 Measurement results . . . 55
4.5 Possible effects that prevented the proper antenna performance . . . 56
4.6 Comparison between measurements vs simulations . . . 61
4.7 New prototype with corrected issues . . . 62

5 Conclusions and future works **65**
5.1 Conclusions 65
5.2 Future works 66

References **67**

Glosary of symbols

Symbol	Name	Unit
a	Radius of cylinder	m
$\vec{A}$	Magnetic vector potential	Wb/m
b	Dimensions of the straight edge of the antenna	m
C	Capacitance	F
D	Antenna directivity	dB
$EIRP$	Equivalent isotropic radiated power	W
f	Frequency	Hz
$\vec{F}$	Electric vector potential	Q/m
G	Antenna gain	dB
h	Thickness substrate	m
$J_n(x)$	Bessel function of first kind of order n	
k	Wave constant	
K_{SR}	Multiplicative correction factor	
L	Inductance	H
$N_n(x)$	Neumann function of first kind of order n	
P_{IC}	Chip sensitivity	W
Q	Quality factor	
R_a, R_{chip}	Antenna and chip resistance	Ω
R_{RMS}	Conductor roughness	$\mu mRMS$
$\|S\|^2$	Power reflection coefficient	dB
$tan\delta$	Loss tangent	
λ	Wavelength	m
θ	Antenna radius of curvature	$degree$
α	Attenuation constant	Np/m
β	Phase constant	Rad/m
δ	Skin depth	m
τ	Transmission coefficient	dB
Ψ	Wave function	

Symbol	**Name**	**Unit**
ϵ_r	Relative Permittivity	ϵ/ϵ_o
$\dot{\epsilon}$	Complex Permittivity	F/m, $(\dot{\epsilon} = \epsilon' - j\epsilon'')$
μ	Permeability	H/m
μ_r	Relative permeability	μ/μ_o
ΔR	Factor of conductor roughness	
V_r	Wave velocity	m/s
X	Inductance	H
W	Width of the antenna	m
Z	Impedance	Ω
(x, y, z)	Rectangular coordinates	
(ρ, ϕ, z)	Cylindrical coordinates	

List of Figures

1.1. Basic components of the passive RFID tag. 2

2.1. Original RFID tag antenna model seen from: a) front view, b) front view with substrate, c) side view. d) Proposed RFID antenna seen from side view. . . . 7
2.2. Reflection coefficient of the tag antenna for a variation of the substrate thickness. 8
2.3. Variation of antenna gain and radiation efficiency in function of the substrate thickness. 9
2.4. Curves on antenna and chip impedances and read range of the tag antenna [1]. 10
2.5. T-matching network configuration. 11
2.6. T-matching structure equivalent circuit model. 11
2.7. Equivalent circuit of tag antenna with T-matching network. 12
2.8. Current distribution of the dipole antenna with (a) T-match network and (b) simple configuration. 13
2.9. Reflection coefficient of the tag antenna for a variation of the parameter p related to the T-match network. 14
2.10.Circuit model of RFID passive tag. 16
2.11.Geometry of the antenna bending on cylindrical surface. 18
2.12.Geometry of the cylindrical cavity seen from side view. 19
2.13.Flowchart of the main steps applied in this work to obtain the best antenna performance. 22

3.1. Resistance of the optimized tag antenna over a copper plate of 125 x 125 mm^2. The chip resistance is also shown. 24
3.2. Reactance of the optimized tag antenna over a copper plate of 125 x 125 mm^2. The conjugate reactance of the chip is also shown. 25
3.3. Power reflection coefficient for the optimized tag antenna attached on flat metallic object of 125 x 125 mm^2. 25
3.4. Gain of the optimized tag antenna on flat metallic object of 125 x 125 mm^2 in the XZ plane (ϕ=0°) and YZ plane (ϕ=90°). 26
3.5. Read range for the optimized tag antenna attached on flat metallic object of 125 x 125 mm^2. 26
3.6. Current distribution for copper plate of: (a) 75 x 75 x mm^2, (b)100 x 100 mm^2, (c)125 x 125 mm^2, (d)150 x 150 mm^2, (e) 175 x 175 mm^2 27
3.7. Read range of the tag antenna over copper plates with different dimensions. . 28

3.8. Resistance of the optimized tag antenna over a copper cylinder of radius=20 mm. The chip resistance is also shown. 29
3.9. Reactance of the optimized tag antenna over a copper cylinder of radius=20 mm. The conjugate reactance of the chip is also shown. 29
3.10.Power reflection coefficient for the tag antenna attached on copper cylinder of radius=20 mm. 30
3.11.Gain of the proposed tag antenna on cylindrical metallic object with radius=20 mm in the XZ plane (ϕ=0°) and YZ plane (ϕ=90°) using genetic algorithm. 31
3.12.Read range for the tag antenna attached on copper cylinder of radius=20 mm. 31
3.13.Current distribution for copper plate of height of 120 mm and radius of: (a)15 mm, (b)20 mm, (c)25 mm, (d)30 mm, (e)35 mm, (f)40 mm 33
3.14.Read range of the tag antenna over cylindrical metallic objects with different radii. 34
3.15.Fitness value of the genetic algorithm used to optimization procedure for a copper cylinder with radius=20 mm. 35
3.16.Resistance of the optimized tag antenna over a copper cylinder of radius=20 mm. The chip resistance is also shown. 36
3.17.Reactance of the optimized tag antenna over a copper cylinder of radius=20 mm. The conjugate reactance of the chip is also shown. 36
3.18.Power reflection coefficient for the optimized tag antenna attached on copper cylinder of radius=20 mm. 37
3.19.2D and 3D radiation pattern of the tag antenna over metallic cylinder with radius=20 mm. 38
3.20.Read range of the optimized tag antenna attached on metallic cylinder with radius=20 mm. 39
3.21.Transmission efficiency and gain of the tag antenna over cylindrical metallic objects with different radii. 39
3.22.Directivity of the tag antenna over cylindrical metallic objects with different radii 40
3.23.Read range of the tag antenna over cylindrical metallic objects with different radii. 40
3.24.Variation of read range in function of power transmission coefficient and gain. The red color represents a maximum read range and the blue color a minimum coverage. 41
3.25.Resistance of the optimized tag antenna over a empty PET bottle of radius=20 mm. The chip resistance is also shown. 43
3.26.Reactance of the optimized tag antenna over a empty PET bottle of radius=20 mm. The conjugate reactance of the chip is also shown. 43

3.27.Gain of the proposed tag antenna on empty PET bottle with radius=20 mm in the XZ plane (ϕ=0°) and YZ plane (ϕ=90°). 44
3.28.Directivity and radiation efficiency of the tag antenna over PET cylinder with different radii. 44
3.29.Read range of the tag antenna mounted on empty PET bottle with radius=20 mm. 45
3.30.Read range of the tag antenna on empty PET bottles with different radii. . . 46
3.31.Read range of the tag antenna on PET bottle of radius=20 mm with different liquid contents. 47
3.32.Directivity and radiation efficiency of the tag antenna over PET bottle of radius=20 mm with different liquid contents. 48
3.33.antenna performance on PET bottle with different kind of liquids. 49

4.1. Two-port network representation of the dipole antenna. 51
4.2. (a) Two-port network and (b) T-network equivalent 52
4.3. Configuration of the test fixture to measure the dipole impedance. 53
4.4. Test fixture used to develop the measurements. 53
4.5. a) Measurement developed in anechoic chamber, (b) prototype built. 55
4.6. Measured and simulated reflection coefficient of the tag antenna. 56
4.7. Reflection coefficient of the antenna for a variation of the parameter b. . . . 57
4.8. Reflection coefficient of the antenna modeled as PEC and copper. 58
4.9. Propagation velocity wave on different surfaces 58
4.10.Reflection coefficient of the antenna for a variation in the electrical properties of the substrate. 61
4.11.Comparison measurements vs simulations for reflection coefficient of the tag antenna attached on copper cylinder with radius=20 mm. 62
4.12.Measured and simulated reflection coefficient of the corrected tag antenna. . 63
4.13.Simulated read range of the corrected tag antenna. 64

List of Tables

2.1. Parameters and dimension of the proposed tag antenna [2]. 6
2.2. Restrictions of the input variables in the genetic algorithm. 17

3.1. Parameters and dimension of the tag antenna mounted on a copper plate using genetic algorithm. 24
3.2. Simulated results of the tag antenna wrapped over copper plates with different dimensions at 915 MHz. 28
3.3. Simulated results of the tag antenna wrapped over cylindrical metallic objects with different radii at 915 MHz. 32
3.4. Parameters and dimension of the tag antenna mounted on a copper cylinder using genetic algorithm 35
3.5. Simulated results of the tag antenna wrapped over cylindrical metallic objects with different radii at 915 MHZ. 38
3.6. Parameters and dimension of the tag antenna mounted on a PET cylinder using genetic algorithm. 42
3.7. Simulated results of the tag antenna on empty PET bottles with different radii at 915 MHz. 45
3.8. Simulated results of the tag antenna on PET bottle of radius=20 mm with different liquid contents at 915 MHz. 47

4.1. Parameters and dimension of the corrected tag antenna mounted on a copper cylinder using genetic algorithm. 63

1 Introduction

Radio Frequency Identification (RFID) is a wireless communication system employed for tracking multiples objects using RF signals. For example, in medical and construction area, it is required the constant supervision and care of instruments, equipment, inventory, and user and technical documents stored in racks and servers with the aim to supply an optimum and innovative service. Also, this technology is very useful for tracking of small metallic items such as: hardware tools, kitchenware, tin cans and spray bottles. Additionally, controlled access to restricted areas requires a reliable security system which can include the use of bracelets and cards equipped with RFID technology.

Sixty years after the publication of its principle of operation [3] (communication by reflected waves), RFID technology remains among the « top ten » worldwide technologies. This growing interest is basically due to the advantages of this technology which provides an automatic, fast, and effective service for applications related to the tracking of objects inside a specific coverage radius. Also, its potential to collect and compile massive amounts of detailed real-time data about its surrounding environment opens the way for plenty of new applications in the field of Internet of Things (IoT) with 50 billion connected objects expected for 2020 [4, 5].

RFID system is mainly composed of three elements: reader, tag and host. The tag comprises an antenna and a chip IC (Integrated circuit) which contains its own identification code (ID). The chip must be energized, in passive or active way, to listen to the commands supplied by the reader and to answer by emitting electromagnetic waves.

The passive tag uses the incident wave sent from the reader to power the chip. After, in the chip IC, it is developed a rectification process of the incident signal, and its complex input impedance is automatically modified to generate the modulated backscattering signal, This process is needed to send back its identification toward the reader [1, 2], as shown in Figure **1.1**, where the performance of the UHF passive RFID system is illustrated.

Furthermore, the host is connected to the reader, working as a data management system and reading the information about the labeled objects. Finally, it develops the data delivery toward the final user.

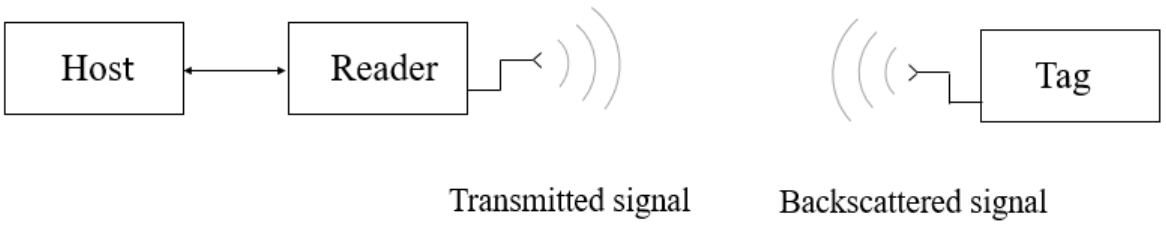

Figure 1.1: Basic components of the passive RFID tag.

Most of RFID systems operates at UHF (Ultra High Frequency) band. The operating frequency varies in each country according to its radio frequency spectrum regulation. Worldwide there are three main frequency bands, the 865-868 MHz band is adopted in Europe, in America the 902-928 MHz band is used, Japan and some Asian Countries use the 952-954 MHz band [1].

It is a hard and challenging task to design antennas fulfilling the operation frequency requirements imposed for RFID applications with an optimum performance over metallic curved surfaces. Improving the read range of the tag is the most important challenge in RFID systems. It requires the assessment of main electrical parameters of the tag antenna, such us: directivity, radiation efficiency, gain, impedance and transmission coefficient to compute the impedance matching with the chip IC.
In literature exists some antenna projects with RFID applications on flexible structures. [2] and [6] propose a small and flexible tag antenna using a ceramic (BaTiO) polymer (polydimethylsiloxane) composite substrate. The flexible substrate has a high-permittivity property in order to reduce the size of the tag antenna and improving its performance.

Moreover, [7] develops a passive UHF RFID tag, designed on an inexpensive paper substrate. In this reference, a cost effective solution to monitor moisture in an absorbing substrate is investigated. The main characteristic of the antenna design is the sensitivity of the antenna polarization on the passive RFID tag to the moisture content in the paper substrate. By simulations, the antenna is circularly polarized when the substrate is dry and the antenna is linearly polarized when the substrate is wet.

In addition, [8] propose a low cost and a low profile flexible microstrip patch tag antenna for UHF RFID systems that can be metal mountable, using a sheet of Teflon with thickness of 0.5 mm as dielectric substrate. The antenna performance over metallic plates is evaluated

by simulations and measurements about impedance, gain and reflection coefficient of the tag antenna.

Finally, [9] proposes a Microstrip Patch Antenna designed for narrow band for materials with three different substrate permittivity. In this work, materials such us: dacron fabric, woven fiberglass fabric and Fleece fabric are used as antenna substrates in order to analyze the antenna's impedance matching and radiation pattern in function of substrate permittivity and the antenna bending.

Small antenna can be defined by Wheeler [10] as a radiator sensor whose maximum dimension is less than the radian-length, in other words, less than 0.5π wavelength. These antennas have a behavior of lumped capacitance or inductance, and the reduction of its size imposes a decrease on the bandwidth due to mismatch (from generator to antenna or from antenna to load) generating a loss of coupling efficiency. By definition, electrical small antennas presents a high quality factor [11]. That means that the antenna has a reduced bandwidth and a limited radiation efficiency. These consequences generate a low antenna gain and limits the tuning of its frequency band, making it difficult the antenna design with a small electrical size.

One of the most important challenges in RFID industry is the antenna design for its operation on materials with high-dielectric constant or high conductivity [12]. These objects degrade the tag performance because the impedance matching between the antenna and the chip is affected, leading to low read range rates [13]. The proximity of the tag and conductive surfaces generates image current which can cancel the antenna current due to the phase difference about 180° between them. This problem can be very damaging because generally the environment is surrounded by metallic objects, which can affect the input impedance, the resonant frequency, gain, efficiency, and radiation pattern of the RFID tag antenna [6, 14]. Furthermore, in RFID tag design, it is very important to propose strategies to reduce the induced current on conductive edges of the object where the tag is wrapped. Generally, when the tag operates over a metallic surfaces, there is a surface current density stored on the edges of the metallic surface which affects the radiation pattern and the antenna efficiency [2].

Moreover, the effect of the antenna curvature plays an important role in the antenna performance. The resonance frequency and the antenna gain are two sensitive electrical parameters to antenna bending [15, 16]. Therefore, the read range and the operating frequency of the tag antenna differ according to the shape of the labeled object.

As it was mentioned, most of published papers on RFID flexible tag antenna in the literature, propose building flexible substrates composed of polymer materials over a cylindrical metallic surface [2, 6, 17]. However, the use of these "homemade"substrates present many disadvantages. First of all, it is not possible to get these kind of materials in the market

easily. Also, the homemade substrate does not provide accurately its electrical parameters. This is due to the measurement procedure of the permittivity and loss tangent not be described in details to determine its reliability. Finally, the manufacturing process is unknown and it can not keep quality standards to guarantee good performance of the product.

Moreover, the paper [2] in addition to use a homemade substrate, does not present a methodology for the antenna design, neither it defines a selection criteria of the antenna parameters. These factors, together the lack of analytic analysis to determine the effect of the antenna curvature on the electrical antenna parameters, represent a limitation in the understanding and contribution of the original proposal.

In such a way, this research proposes a RFID tag for mounting on curved metallic surfaces. The tag comprises the small antenna design at UHF band, using a flexible commercial substrate. The starting point is the tag antenna originally proposed in [2]. In this work, its design parameters are modified using a genetic algorithm to optimize its performance. The optimization process is based on the manipulation of the parameters which involve the T-matching network, the size of the slots and the dielectric loading to improve the antenna performance.

Then, the main contribution of this project is proposing a RFID flexible tag antenna in the UHF band for applications which involve curved metallic structures, using a commercial flexible substrate. The proposal provides an optimized methodology for antenna design, using an optimization process which defines an optimum geometry of the antenna to improve its performance. The antenna performance evaluates the following parameters: return loss, impedance matching between the antenna and chip, gain, and read range. Moreover, an analytic analysis about the effects of the antenna curvature based on the cylindrical cavity model is developed to determine the influence of this variable in the resonance frequency of the antenna. Finally, the influence of the substrate thickness and the roughness effect on its electrical parameters is analyzed, with the aim to have a good precision in the properties of substrate permittivity and dielectric loss, allowing the proper design of RFID small antennas.

Furthermore, in this work an optimal tag antenna is designed with a maximized read range, when mounted on plastic (polyethylene terephthalate - PET) bottles. Additionally, the electromagnetic behavior of the tag antenna on PET cylinders is evaluated with different liquid contents.

1.1. Objectives

The main objective of this work is to design a passive UHF RFID tag using a commercial flexible substrate. Also, this research proposes a project methodology for antenna design considering the surface curvature where the antenna is placed.
Based on the general objective, the following specific objectives were defined:

- Selecting the flexible substrate with optimum electrical characteristics.
- Simulating the tag antenna in HFSS software and evaluating its electromagnetic performance.
- Studying the effect of antenna curvature on its electromagnetic performance.
- Optimizing the geometry of the tag antenna by maximizing its read range.
- Building the RFID tag prototype and developing measurements about antenna impedance and reflection coefficient.
- Analyzing and comparing the antenna performance in the simulated and measured scenario.

2 Antenna Design and Methodology

2.1. Antenna Characteristics of the original work

The geometry of the tag antenna designed in this work is shown in Figure **2.1**. The antenna has a dimension of W=13 mm x L=28 mm. The tag is equipped with NXP G2iL IC chip [18]. It has a complex impedance of 23-j224 Ω at the central frequency of 915 MHz [19]. Besides, the chip has a sensitivity P_{IC}=-18 dBm.

Figure **2.1** displays the original tag antenna seen from a front and side view (a, b, c). Also, it is illustrated in (d) a proposed modification in the antenna substrate to achieve an optimum performance. The antenna substrate has a cylindrical geometry with radius=16 mm. Table **2.1** shows the parameters and dimensions of the tag antenna originally proposed by [2], using a homemade substrate fabricated with a high-dielectric polymer-ceramic composite substrate ($BaTiO_3$ + polydimethylsiloxane polymer), with dielectric constant about 12 and loss tangent close to 0.01.

However, the substrate used in the original proposal is a homemade material. Then, its acquisition in the market is not possible and its electrical parameters, as permittivity and loss tangent, are not provided with a high accuracy by the manufacturer.

Table 2.1: Parameters and dimension of the proposed tag antenna [2].

Parameter	**Length (mm)**	**Parameter**	**Length (mm)**	**Parameter**	**Length (mm)**
a	3	f	6	n	1
b	2	g	5	o	11
c	1	h	1.5	p	6
d	2	i	1	L	28
e	1	m	1.5	W	13

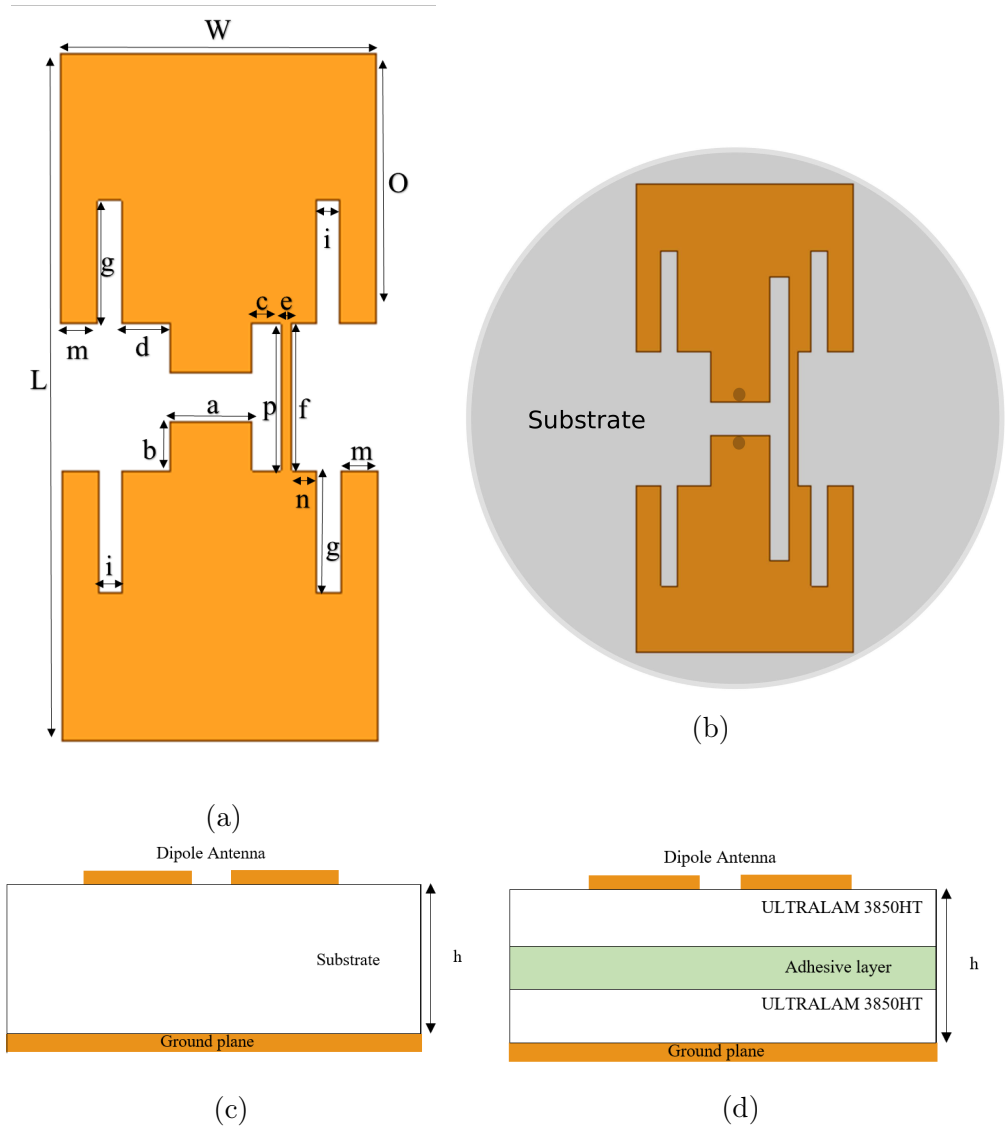

Figure 2.1: Original RFID tag antenna model seen from: a) front view, b) front view with substrate, c) side view. d) Proposed RFID antenna seen from side view.

2.2. Selection of the substrate

According to the disadvantages using a homemade substrate, it was defined a selection criteria of a new substrate based on the following items: acquisition in the market, good performance in high frequencies, a high dielectric constant and a low dielectric loss.

Thus, based on the searching in the market and considering the selection criteria, it was selected the Rogers Ultralam 3850HT substrate with the following characteristics: dielectric constant of 3.14 and dielectric loss tangent of 0.002 [20].

The use of the selected substrate on the original antenna, with dimensions 13 mm x 28 mm, presents a displacement of the resonance frequency in the gigahertz order. Nevertheless, it is desirable to achieve an impedance matching between the chip IC and the tag antenna at 915 MHz frequency band. Thus, the selection of a substrate with high dielectric constant allows a decrease in the resonance frequency of the antenna and obtaining a proper impedance matching in the desired frequency band [11].

Furthermore, the substrate thickness was chosen based on the antenna performance for the selected application. Rogers Corporation supplies three different substrate thickness: 0.025 mm, 0.05 mm, 0.1 mm and 0.175 mm. Hence, simulations to determine the electrical performance for each case were run, in order to select the proper thickness. Here, parameters as: resonance frequency, radiation efficiency and antenna gain, differ depending on the selected thickness. In this work, the radiation efficiency and antenna gain were computed without considering the reflection coefficient due to impedance matching. Then, it was concluded that, as the substrate thickness increases, the radiation efficiency, antenna gain and resonance frequency increase too, as depicted in Figure **2.2** and **2.3**. However, the impedance matching tends to worsen.

Based on the analysis of the cavity model with loss for microstrip antennas in [21], the increment of the quality factor, which occurs for an increase of the substrate thickness, produces an increment in the resonance frequency of the antenna.

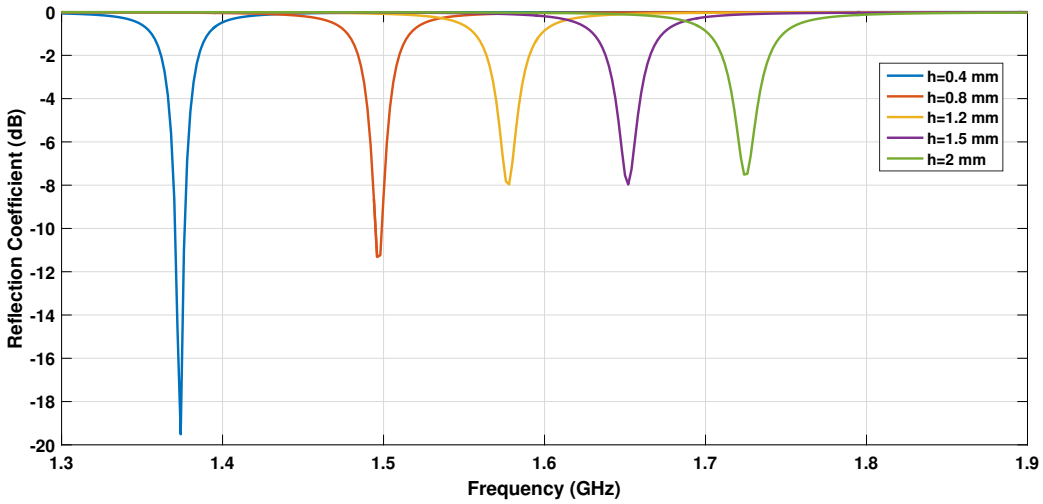

Figure 2.2: Reflection coefficient of the tag antenna for a variation of the substrate thickness.

In such a way, a substrate thickness which presents an optimal balance among the mentioned electrical parameters, was needed to achieve good antenna performance. Here, a substrate

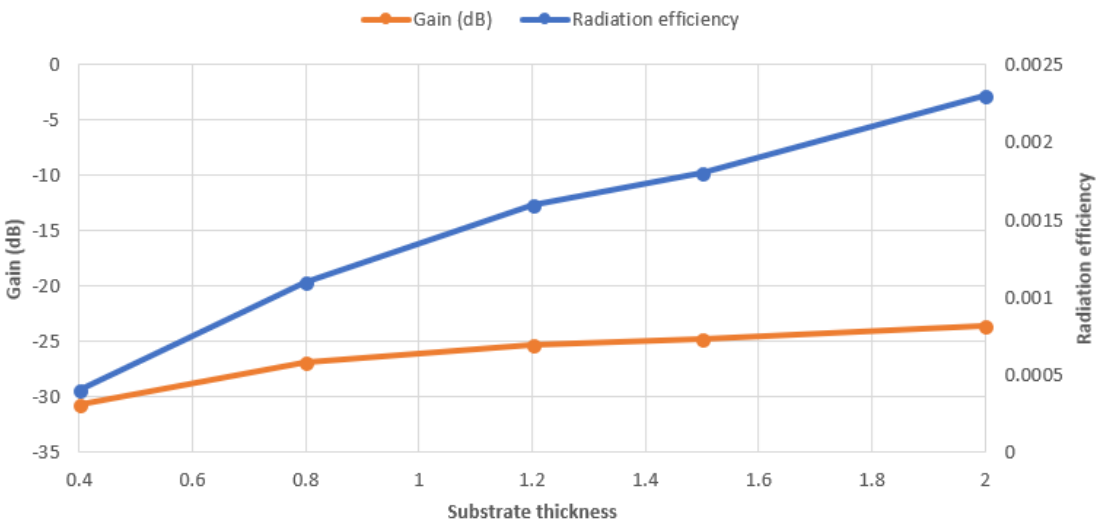

Figure 2.3: Variation of antenna gain and radiation efficiency in function of the substrate thickness.

laminate with the highest thickness does not satisfy an optimal antenna performance. Then, two laminates of Ultralam 3850HT (each laminate with thickness of 0.175 mm) with an adhesive layer were selected to create a single substrate with thickness of 0.4 mm [20, 22], as shown in Figure **2.1 d)**.

2.3. Characteristics of the selected tag antenna

Figure **2.4** shows a graphical representation of the main electrical characteristics of a RFID tag [1], where R_a and X_a are the antenna resistance and reactance, and R_c and X_c are the chip resistance and reactance. Parameters such as: antenna input impedance, chip impedance, resonance frequency, read range and the range bandwidth of the tag antenna, are very important to analyze the electrical performance of the selected antenna. Here, bandwidth may be defined as the frequency band in which the tag can generate a minimum required range produced by the backscattering process with the aim that the reader can demodulate and accept the signal information provided [1].

In order to accomplish good matching impedance among chip and antenna, it is very important to adjust the antenna reactance in the desired frequency, which can be improved through the addition of slots and T-matching networks [13]. A good matching leads to maximum power transfer, and consequently, a high transmission coefficient.

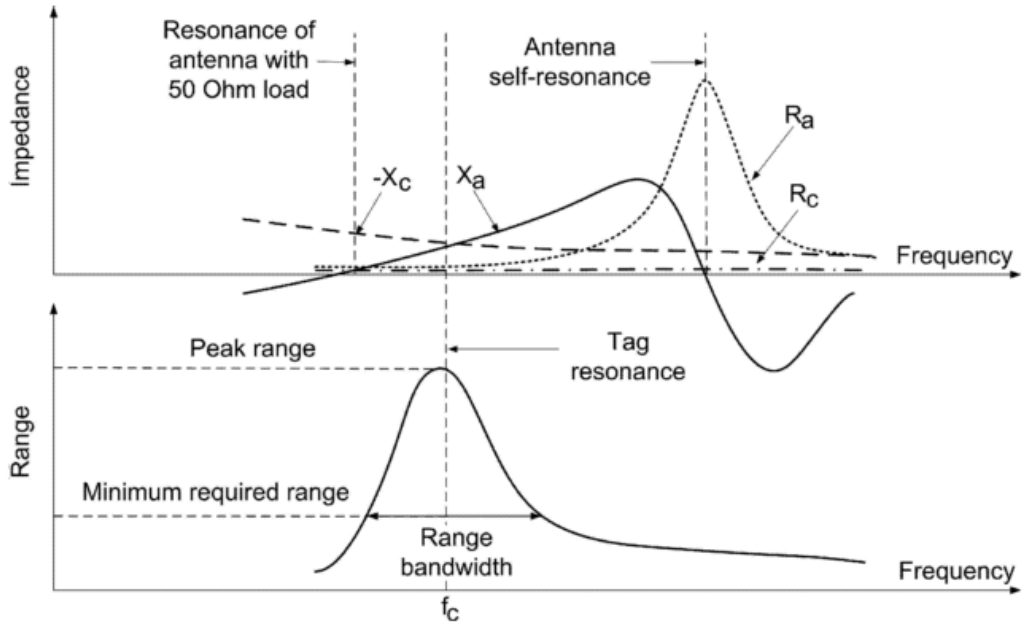

Figure 2.4: Curves on antenna and chip impedances and read range of the tag antenna [1].

Equation (2.1) shows the relation between the resonance frequency and the antenna reactance for an equivalent RLC circuit. An increase of the antenna reactance, through its capacitance and inductance, produces a reduction in its resonance frequency, which, in many cases, is the goal, so as to minimize the overall size of the antenna or to achieve a good impedance matching.

$$2\pi f = \sqrt{\frac{1}{LC}} \tag{2.1}$$

The selected dipole antenna is composed of two main combinations that involve techniques to miniaturize the geometry of the antenna and reach good performance. These elements are T-matching and slots.

2.3.1. T-matching

T-matching network is an important method in small antennas design to achieve an impedance matching between the chip and tag antenna. In this case, the input impedance of the planar dipole is modified by introducing a centered short-circuit stub, as shown in Figure **2.5**. T-matching adds a conductor loop in the antenna structure around its terminals, where the slot generates a short circuit current path. Hence, the slot controls the current path, and

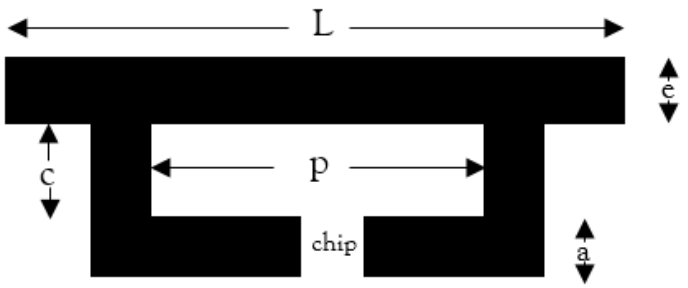

Figure 2.5: T-matching network configuration.

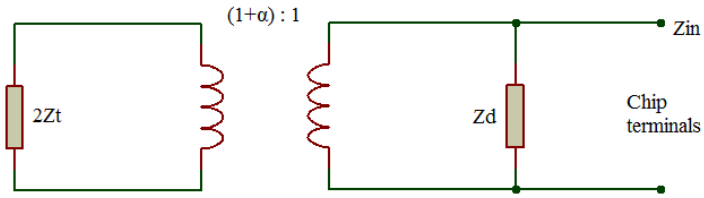

Figure 2.6: T-matching structure equivalent circuit model.

therefore, the inductive impedance of the antenna through the shape of the stub [23].

Figure **2.6** displays an equivalent circuit of a typical dipole with a T-match configuration. This network modifies the antenna impedance to the desired frequency through the adjustment of T-match geometry [24]. The structure can be represented by an equivalent circuit, where the T-match works as an impedance transformer, which, depending on the transformation relation can provide a good matching impedance and reduce the overall size of the tag antenna [2, 21].

Where:

- Zt: Impedance of shorted-circuit formed by the T-matching and dipole.
- Zd: Dipole impedance in the absence of T-match connection.

T-matching has a degree of freedom represented by "α", which defines the matching relation between the antenna and chip impedance. Additionally, the matching factor (α) determines the current division factor between the two conductors, as given in equation (2.2).

$$\alpha = \frac{\log\left(\frac{c+\frac{a}{2}+\frac{e}{2}}{a'}\right)}{\log\left(\frac{c+\frac{a}{2}+\frac{e}{2}}{e'}\right)} \tag{2.2}$$

For e'=0.5e and a'=0.5a. These variables are the equivalent radii of the dipole antenna and the matching stub, respectively.

Equation (2.3) represents the impedance at the source point as a function of α. The optimum adjustment of parameters a, c, e and p, implies an increase of the antenna impedance (Z_{in}) and a shift of the resonance frequency of the tag.

$$Z_{in} = Z_{chip}* = \frac{2Z_t[(1+\alpha)^2 Z_d]}{2Z_t + (1+\alpha)^2 Z_d} \tag{2.3}$$

Where the input impedance of the short-circuit stub (Z_t), represents the T-match conductors and part of the dipole antenna, and depends on the characteristic impedance of the two-conductor transmission line (Z_o), with spacing $c + \frac{a}{2} + \frac{e}{2}$.

Furthermore, the tag antenna with T-matching network can be represented by the equivalent circuit of Figure **2.7**. The T-match is composed of shunt and series inductances which allow the impedance matching with the high capacitive chip impedance [14], adjusting the vertical and the horizontal length of the T-match, through the parameters p and c.

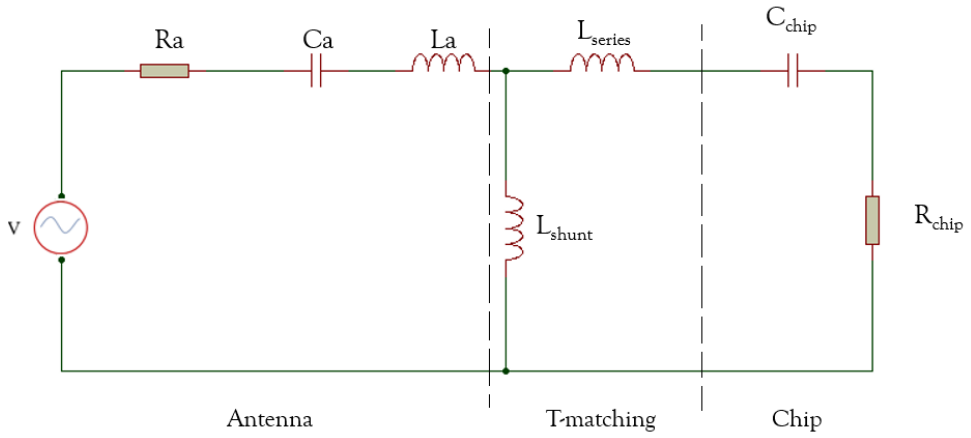

Figure 2.7: Equivalent circuit of tag antenna with T-matching network.

The antenna configuration without the T-match network (see Figure **2.8 b**) has an approximate impedance of 0.04+6.9j Ω at 915 MHz. Therefore, the T-match network plays an

important role in the impedance matching between the antenna and chip [25], by increase the inductive impedance of the tag antenna. This matching leads to maximum power transfer and a reduction of its operation frequency, satisfying good antenna performance and high radiation efficiency.

Figure **2.8** shows the current distributions of the tag antenna, with and without the T-match network. The amplitude of the surface current density is concentrated around the T-match network as consequence of the addition of inductive loads to the dipole antenna. This allows increasing the antenna impedance and helps achieving an optimum impedance matching between the chip and antenna. In the absence of the T-matching, the current density is diminished on the antenna surface, representing less power in the tag antenna to radiate the backscattering signal towards the reader.

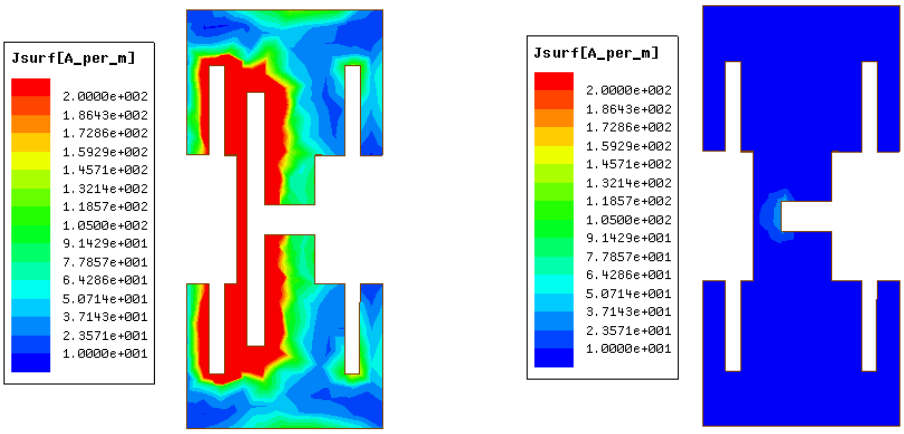

(a) (b)

Figure 2.8: Current distribution of the dipole antenna with (a) T-match network and (b) simple configuration.

As was analyzed in this section, the parameter p is a sensible variable influencing the performance of the antenna. Figure **2.9** illustrates the power reflection coefficient of the tag antenna, with the selected parameters in section 3.2.1, changing the geometry of the T-match network when the antenna is mounted on copper plate of 125 mm x 125 mm. An increment of parameter p produces an increase in the antenna inductance, and therefore, the reduction of the resonance frequency. Additionally, the return loss decreases at 915 MHz frequency for high values of p.

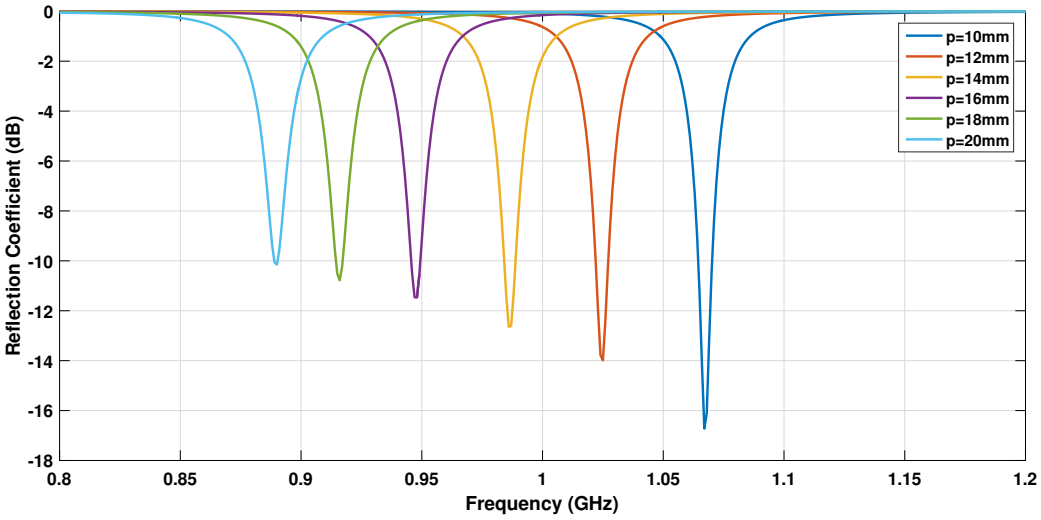

Figure 2.9: Reflection coefficient of the tag antenna for a variation of the parameter p related to the T-match network.

2.3.2. Shaped slots

One of the most feasible strategies to achieve the complex impedance matching is the employment of shaped slot which produce a high inductive reactance in the antenna. The slot can be represented as an impedance transformer, where each discontinuity supplies energy storage and radiation. For this reason, each discontinuity can be considered as a further degree of freedom, and it is very important to execute tasks related with miniaturization and impedance matching in a specific resonance frequency [24].

Moreover, for small antennas, the current flows from one edge towards the other. However, when the slots are located on the antenna, the current is blocked, representing a high impedance path. Thus, the current requires a longer path to reach the other antenna edge, increase the series inductance [24]. Consequently, the current density tends to increase in surrounding areas of the slot due to the high current flux.

The analysis of its electromagnetic behavior can be done through the equivalent circuit of the slot with a typical RLC. Therefore, depending on the shape and size of the internal slot is possible to obtain a high peak reactance and to achieve the antenna tuning in the desired frequency.

As the size of the slot's width increases, the resonance frequency and the peak reactance are reduced [24], produced by increase capacitances of the antenna. Additionally, the resistance is sensitive to the slot's width, while the reactance has fast and nearly linear variations to

the size of slot's width and length.

Thus, slots play an important role in antenna tunning in the desired operating frequency based on the increase of the current path [26]. Nevertheless, if the size of the slot is too large, it can serve as a significant obstruction in the flow of resonant fields and currents, producing undesired reflections [11]. The size reduction of the tag antenna is limited by the amount of parasitic inductance which are introduced by the slot segments [27].

The power reflection coefficient and resonance frequency of the tag antenna can be adjusted with a variation on slot's parameter g of the tag antenna [2]. The increase of the slot through the parameter g in the dipole structure generates a decrease of the operating frequency.

2.4. Optimization problem

For improving the antenna performance, the main challenge in RFID systems is to maximize the tag read range. Hence, to satisfy this goal, a maximum power transfer between antenna and chip is needed, and to enhance the antenna gain. This aim wants to accomplish a good transmission efficiency which allows to generate the backscattering signal by the tag.

Most antennas are designed to operate with an input impedance of 50 Ω or 75 Ω. However, the chip impedance has a complex impedance that varies with the frequency. For RFID tag, it is crucial to achieve suitable impedance matching between the chip and the antenna. In such a way, it is important that the antenna impedance tends to the conjugate of the chip impedance to transfer the maximum power and reach a wide read range [14]. Figure **2.10** shows a simple circuit model for RFID tag [28], where it is possible to analyze the importance of impedance matching.

In order to evaluate the antenna performance, it is useful to know how well the antenna and the chip are matched. Thus, the power transmission coefficient is given by [2]:

$$\tau = \frac{4R_a R_{chip}}{|Z_a + Z_{chip}|^2} \tag{2.4}$$

Where Z_a=R_a+jX_a and Z_{chip}=R_{chip}+jX_{chip} are the complex antenna and microchip input impedances.

The power reflection coefficient $|S|^2$, also named return loss, is defined as the ratio of the incident power on the tag antenna and the power reflected back [2], as shown in equation (2.5).

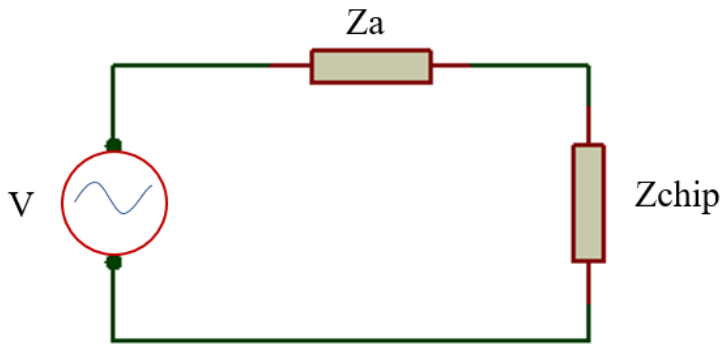

Figure 2.10: Circuit model of RFID passive tag.

$$\frac{P_{ref}}{P_{in}} = \left| \frac{Z_{chip} - Z_a*}{Z_a + Z_{chip}} \right|^2 \tag{2.5}$$

Subsequently, the read range can be defined as the maximum distance at which the reader can detect the tag antenna. The read range can be expressed by the Friis equation: [23]:

$$d_{tag} = \frac{\lambda}{4\pi}\sqrt{\frac{G_{tag}\tau EIRP}{P_{IC}}} \tag{2.6}$$

Where P_{IC} is the chip sensitivity, G_{tag} is the tag antenna gain, τ is the transmission coefficient and EIRP represents the equivalent isotropic radiated power, defined as 4 W at 915 MHz, according to the normative [19]. Also, a polarization matching between the reader and tag is assumed perfect. Then, the polarization efficiency is 1.

In order to achieve the best antenna performance, an optimization process on the geometry of the antenna was applied, using a Genetic Algorithm (GA) [29] by a Matlab's toolbox and HFSS. GA method is a stochastic search algorithm with good characteristics of local search and generation of diversity. GA is used in antenna projects to obtain optimal solutions for many problems, through the evolution of organisms and biological observations [30, 31].

The objective of the optimization was maximizing the read range of the tag in the central frequency of 915 MHz. In the optimization process, firstly it was developed an antenna parametrization, including all parameters of the tag, to determine which antenna parameters are the most sensitive to improve the impedance matching and the antenna gain. In this sense, 6 parameters (a, c, f, g, n, and p according Figure 2.1) were selected, and they were defined as input variables in the genetic algorithm to maximize the read range of the tag on the metallic surface, as shown in Table **2.2**.

Table 2.2: Restrictions of the input variables in the genetic algorithm.

Parameter	**Length (mm)**	**Parameter**	**Length (mm)**
a	$2.5 \leq a \leq 3.5$	g	$5 \leq g \leq 10$
c	$0.8 \leq c \leq 1.2$	n	$0.8 \leq n \leq 1.2$
f	$5 \leq f \leq 10$	p	$12 \leq p \leq 22$

Afterwards, an objective function was defined, considering a reference read range of 5 m to guarantee the proper maximization of read range of the tag. Hence, the objective function $f(x)$ was minimized to achieve the best antenna performance, as shown in the following equation.

$$minf(x) = 5m - d_{tag} \tag{2.7}$$

Moreover, in the GA optimization, a population size of 25 individuals and 10 generations were defined, where the population is submitted to selection, recombination and mutation operators to find the optimum values. Here, it was chosen the selection function roulette, a constraint dependent as recombination and mutation functions, with a recombination fraction of 0.8.

The algorithm initializes the first generation randomly and operates until the last generation where it finds the best antenna parameters to maximize its read range. The selection criteria on the number of individuals and generations was based on the analysis of convergence of the objective function and the execution time of the algorithm. Moreover, in the algorithm, two individuals were selected as elite population, representing almost 10 % of the population, in order to save a record of the best results for each generation.

2.5. Search space of optimization

The small antenna design for RFID systems with application on different surfaces requires a prior knowledge of the electromagnetic behavior of small antennas as a function of the antenna curvature. Thus, the performance of small antennas mounted on curved surfaces can be studied using the cylindrical cavity model. This model provides an approximated electromagnetic analysis for the selected antenna, in order to understand the effect of the

antenna curvature on the resonance frequency and radiation field solution.

Some papers like [16] and [15] analyze the effect of antenna curvature on the characteristics of TM_{10} and TM_{01} modes. They explain the effects of curvature on radiation patterns and input impedances for small antennas. Also, it is demonstrated how the antenna curvature has different effects on the E and H plane patterns.

The following analysis corresponds to the effect of curvature on microstrip antennas, which represents a good approximation for this work because of the geometry and structure of the selected antenna. The main parameters of the antenna bending on a cylindrical surface are shown in Figure **2.11** and **2.12** from different angles, where a is the radius of the cylinder, ϵ_r the substrate relative permittivity, L is the dimension of the straight edge of the tag antenna, h is the substrate thickness, and the curved edge is expressed by $2(a+h)\theta$.

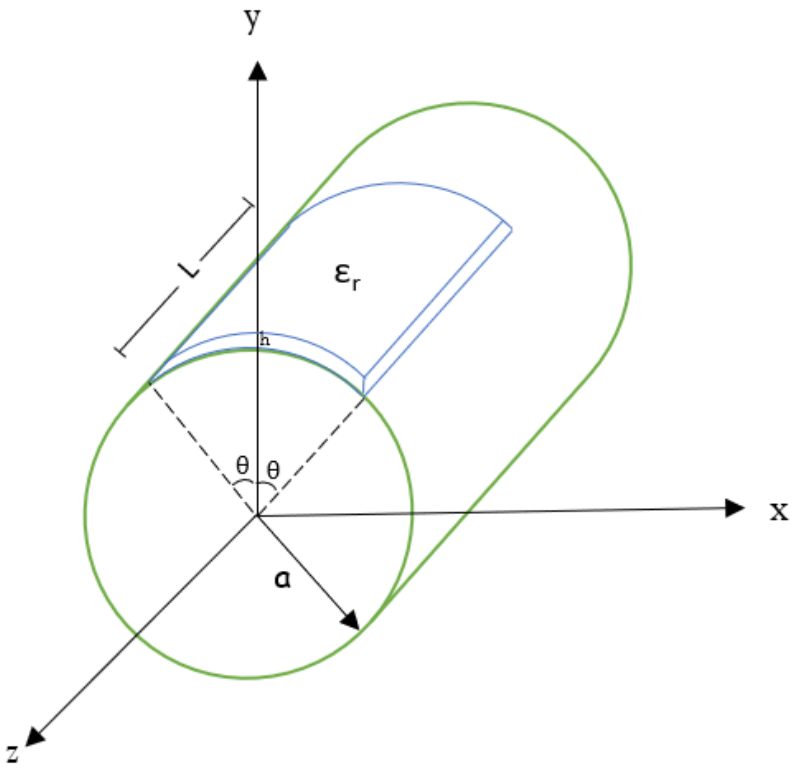

Figure 2.11: Geometry of the antenna bending on cylindrical surface.

The substrate is considered as a cylindrical cavity with electric walls on the top and bottom (conducting antenna and grounded cylindrical surface) and magnetic walls on the side (dielectric cavity). The electric walls are located at $\rho = a, a+h$; and the magnetic walls are located at $z = 0, L$ and $\phi = 0, 2\theta$.

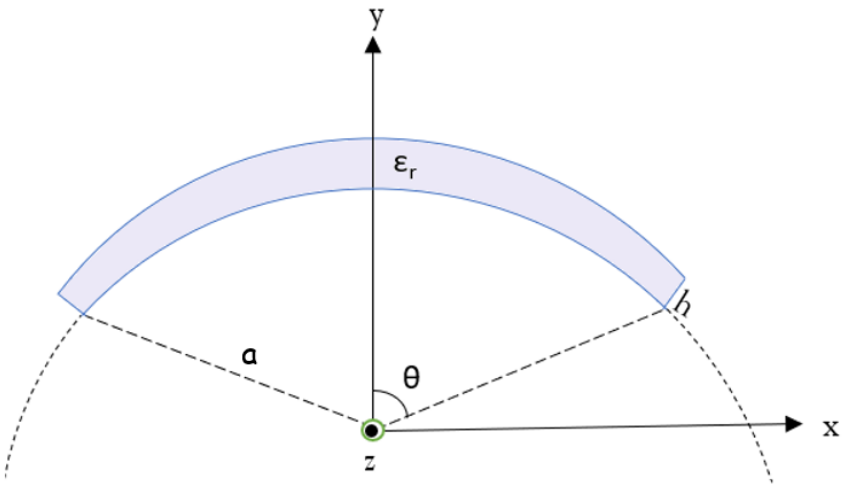

Figure 2.12: Geometry of the cylindrical cavity seen from side view.

The main assumptions that guarantee the existence of the previous consideration in the analysis of cylindrical cavities, is the substrate thickness must be much smaller than the wavelength ($h \ll \lambda$) and it must be much smaller than the radius of the conductive cylinder ($h \ll a$), for small antennas applications [15, 16]. Based on these conditions, only TM modes are assumed to exist [32].

So, the analysis of the cavity model is developed for the transverse magnetic (TM_z) mode to find a relation between the antenna curvature and its resonance frequency. The electric and magnetic fields of the TM mode to z [33] are expressed as:

$$E_\rho = \frac{1}{j\omega\epsilon\mu}\frac{\partial^2\psi}{\partial\rho\partial z} \qquad H_\rho = \frac{1}{\rho\mu}\frac{\partial\psi}{\partial\phi}$$

$$E_\phi = \frac{1}{j\omega\epsilon\mu\rho}\frac{\partial^2\psi}{\partial\phi\partial z} \qquad H_\phi = \frac{-1}{\mu}\frac{\partial\psi}{\partial\rho}$$

$$E_z = \frac{1}{j\omega\epsilon\mu}\left(k^2\psi + \frac{\partial^2\psi}{\partial z}\right) \qquad H_z = 0$$

TM to z field solution can be analyzed as function of its potential vector for mediums with linear, homogeneous, and isotropic characteristics in the absence of sources, where $\vec{A} = \vec{a_z}\vec{\psi}$ and $\vec{F} = 0$. Additionally, the wave function for cylindrical coordinates can be expressed as: $\psi(\vec{r}) = R(\rho)P(\phi)Z(z)$.

The analysis is developed based on the following steps:

a) Applying the boundary conditions on magnetic walls: For θ=0, $2\pi \longrightarrow H_\rho = H_z = E_\phi$=0

$$P(\phi) = \cos\left(\frac{m\pi}{2\theta}\theta\right), m = 0, 1, 2, ... \tag{2.8}$$

b) Applying the boundary conditions on magnetic walls: For $z = 0, L \longrightarrow H_\rho = H_\phi = E_z = 0$.

$$Z(z) = \sin\left(\frac{n\pi}{L}z\right), n = 1, 2, ... \tag{2.9}$$

c) Applying the boundary conditions on electric walls: For $\rho = a, a+h \longrightarrow E_\phi = E_z = H_\rho = 0$.

$$R_v(\rho) = a_1 J_v(k_\rho \rho) + a_2 N_v(k_\rho \rho) \tag{2.10}$$

Where $J_v(k_\rho\rho)$ and $N_v(k_\rho\rho)$ are the Bessel and Neumann function of order v.

It can be written as:

$$a_1 J_v(k_\rho a) + a_2 N_v(k_\rho a) = 0 \tag{2.11}$$
$$a_1 J_v(k_\rho(a+h)) + a_2 N_v(k_\rho(a+h)) = 0 \tag{2.12}$$

d) In such a way, it can be expressed as:

$$\psi_{TMz} = A_{mn} R_v(k_\rho \rho) \sin\left(\frac{n\pi}{L}z\right) \cos\left(\frac{m\pi}{2\theta}\phi\right) \tag{2.13}$$

Where A_{mn} is a constant, and:

$$k^2 = \omega^2 \mu\epsilon = (k_\rho)^2 + \left(\frac{n\pi}{L}\right)^2 \tag{2.14}$$

e) Using cylindrical coordinates, the source-free electric field satisfies the wave equation as follows:

$$\frac{1}{\rho}\frac{\partial \rho E_\phi}{\partial \rho \partial \phi} - \frac{1}{\rho^2}\frac{\partial^2 E_\rho}{\partial \phi^2} - \frac{\partial^2 E_\rho}{\partial z^2} + \frac{\partial^2 E_z}{\partial z \partial \rho} - k^2 E_\rho = 0 \tag{2.15}$$

Following the usual cavity model approximation, the electric field is assumed to have only one component. Then,

$$E_\rho = -\frac{j}{\omega\mu\epsilon} k_\rho \left(\frac{n\pi}{L}\right) A_{mn} R'_v(k_\rho \rho) \sin\left(\frac{n\pi}{L}z\right) \cos\left(\frac{m\pi}{2\theta}\phi\right) \tag{2.16}$$

And,

$$k^2 = \left(\frac{m\pi}{2\theta(a+h)}^2\right) + \left(\frac{n\pi}{L}\right)^2 \tag{2.17}$$

Where:

$$k_\rho = \frac{m\pi}{2\theta(a+h)} \tag{2.18}$$

Finally, the resonance frequency can be written as:

$$f_r = \frac{1}{2\epsilon\mu}\sqrt{\left(\frac{m\pi}{2\theta(a+h)}\right)^2 + \left(\frac{n\pi}{L}\right)^2} \tag{2.19}$$

Equation (2.16) displays the relation of the electric field of the cavity in function of the antenna curvature. Then, an increase of the antenna curvature produces the decrease of the electric field in the cavity, which affects the radiation efficiency of the antenna.

The average dissipated power can be expressed by the following equation:

$$< P_d >= \frac{\omega}{2}|\mathbf{E}|^2\epsilon'' \tag{2.20}$$

Where ϵ'' is the imaginary part of the complex permittivity and it models the dielectric losses of the cavity, which it depends only of the frequency.

Consequently, the decrease of the electric field produces the reduction of the dissipated power in the cavity, which it leads the improving of the radiation efficiency in the antenna. Hence, the antenna gain enhances with the increase of the antenna curvature.

Furthermore, based on equation (2.19), it is possible to observe that the antenna curvature affects the resonance frequency of the tag antenna. An increment of the angle θ generates a slight reduction of the resonance frequency.

These concepts explain how the antenna curvature affects its electromagnetic properties, and why is important to design and optimize the tag antenna for a predefined structure in order to obtain maximum read range. Therefore, if the antenna design for RFID applications on curved surface is desired, the application of optimization directly on the selected geometry to achieve the best antenna performance is suggested.

Figure **2.13** shows a flowchart with the proposed methodology for antenna design, which it is employed for optimizing the original antenna, by maximizing its read range.

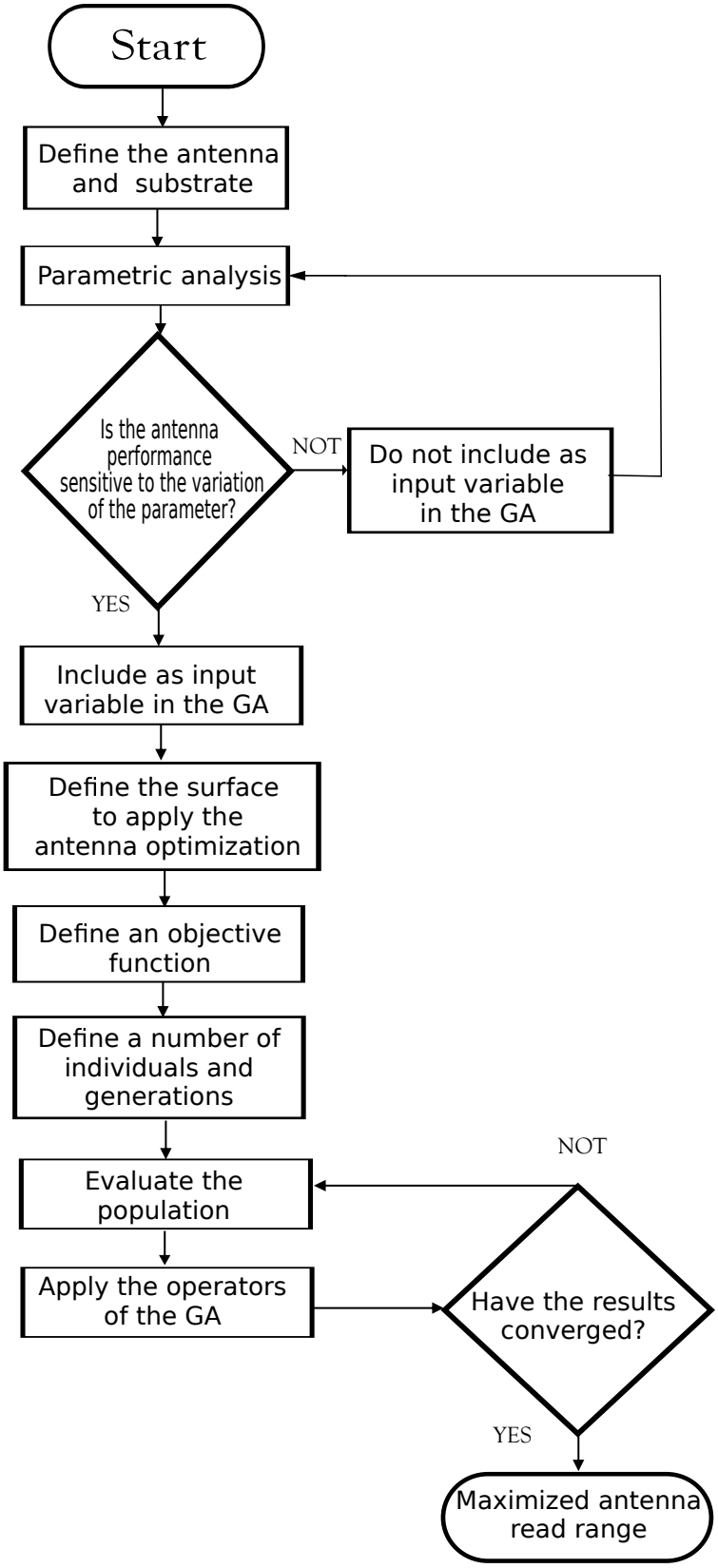

Figure 2.13: Flowchart of the main steps applied in this work to obtain the best antenna performance.

3 Simulation results

3.1. Computational model

The tag antenna is simulated in HFSS v.15 to assess its electromagnetic properties. The conductor of the tag antenna was modeled as Perfect Electric Conductor (PEC) and the substrate as a dielectric (see section 2.2). Moreover, the tag was modeled as an integration of a dipole antenna and a lumped port with complex impedance to model the chip IC. A central frequency of 915 MHz was selected to compute the far field electromagnetic solution of the tag antenna. Then, in this software, the impedance and gain of the tag antenna was simulated, and after, were exported to MATLAB software to compute the reflection coefficient, transmission coefficient and read range of the tag.

3.2. Optimization on copper plate

In this section, the optimization results of the tag antenna mounted on a copper plate of 125 mm x 125 mm are presented. First, the performance of the optimized antenna on flat surfaces is analyzed. After, the antenna performance on cylindrical objects is presented. This organization was selected with the goal to create a project methodology for antenna design.

Table **3.1** presents the parameters of the optimized antenna mounted on copper plate of 125 mm x 125 mm, through the maximization of the read range, using genetic algorithm.

3.2.1. Antenna performance on copper plate

The impedance of the tag antenna on metallic plate is depicted in Figures **3.1** and **3.2**. The antenna impedance at 915 MHz is 13.72+230.2j Ω, and it allows complex impedance matching with the chip to minimize the return loss produced by the reflection of the incident power. Despite the antenna having a proper reactance to achieve matching, the real impedance is not equal to the chip resistance. It generates that the maximum power transfer can be limited because, based on tag equivalent circuit, part of incident power is reflected.

Table 3.1: Parameters and dimension of the tag antenna mounted on a copper plate using genetic algorithm.

Parameter	Length (mm)	Parameter	Length (mm)	Parameter	Length (mm)
a	3.31	f	8.6	n	0.85
b	2	g	6	o	9.7
c	1.2	h	0.4	p	17
d	2	i	1	L	28
e	0.64	m	1.5	W	13

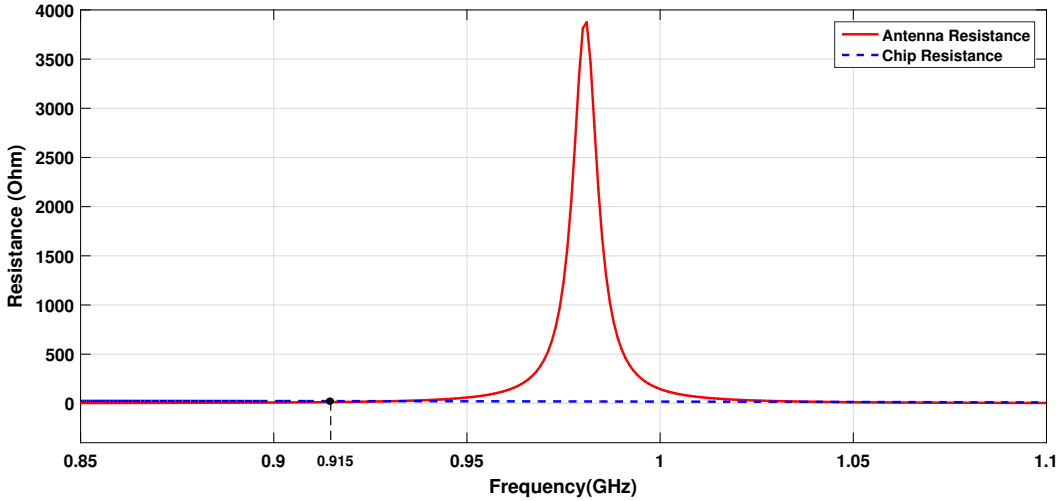

Figure 3.1: Resistance of the optimized tag antenna over a copper plate of 125 x 125 mm^2. The chip resistance is also shown.

Figure **3.3** illustrates the return loss of the tag antenna. The reflection coefficient is -10.45 dB, good value, which represents a power transfer of 91 % of the available power on the antenna terminals. Additionally, the tag antenna on the flat surface has a bandwidth of 19 MHz in the 905 MHz – 924 MHz frequency band, using the criteria of -3 dB [34] to computer it.

Moreover, the antenna gain on copper plate of 125 x 125 mm^2 is depicted in Figure **3.4**. Here, the antenna is placed on the Z-axis. Then, it is possible to observe that the maximum antenna gain is -26.64 dB. The maximum antenna directivity is 2.67 dB and its radiation pattern has a sectoral aspect due to the metallic planar surface, which acts as a ground plane and helps to improve the antenna directivity.

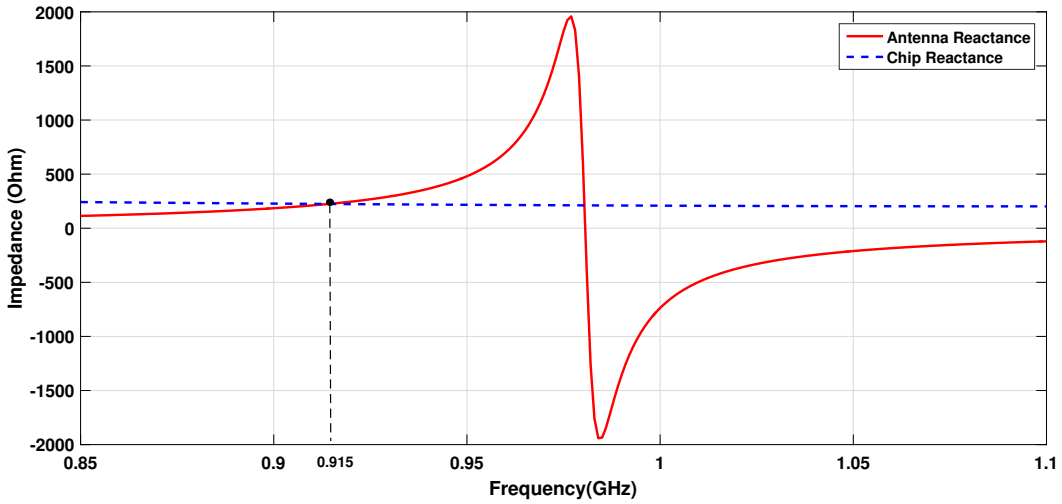

Figure 3.2: Reactance of the optimized tag antenna over a copper plate of 125 x 125 mm^2. The conjugate reactance of the chip is also shown.

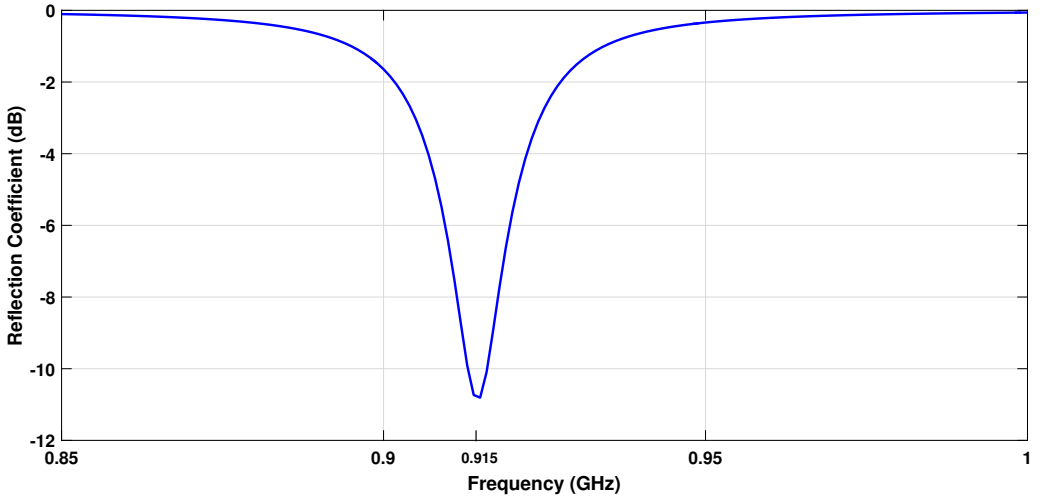

Figure 3.3: Power reflection coefficient for the optimized tag antenna attached on flat metallic object of 125 x 125 mm^2.

The low radiation efficiency of the proposed antenna is generated due to its high quality factor, which it is intrinsic property of small antennas. Therefore, it leads to obtain a low radiation resistance and a low gain.

Figure **3.5** shows the read range of the tag when it is mounted on a copper plate of 125 x 125 mm^2. The read range is 0.58 m at 915 MHz, value very limited for applications related

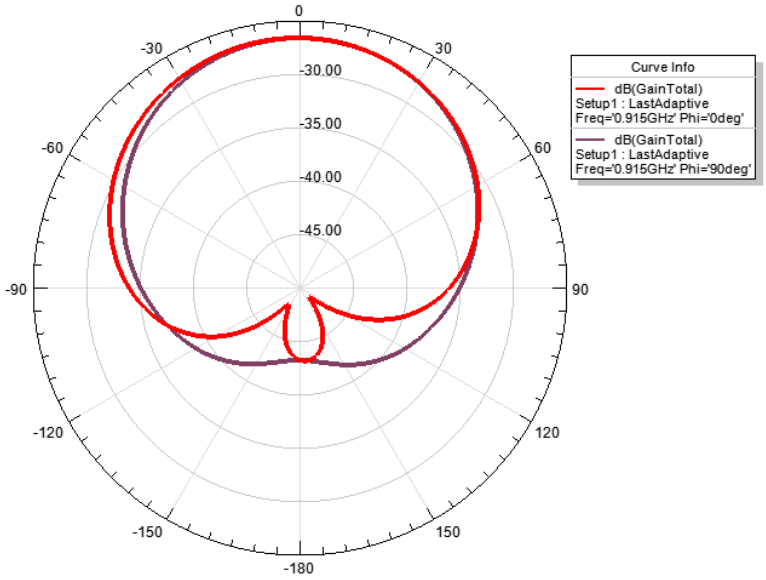

Figure 3.4: Gain of the optimized tag antenna on flat metallic object of 125 x 125 mm^2 in the XZ plane (ϕ=0°) and YZ plane (ϕ=90°).

to tracking metallic flat objects.

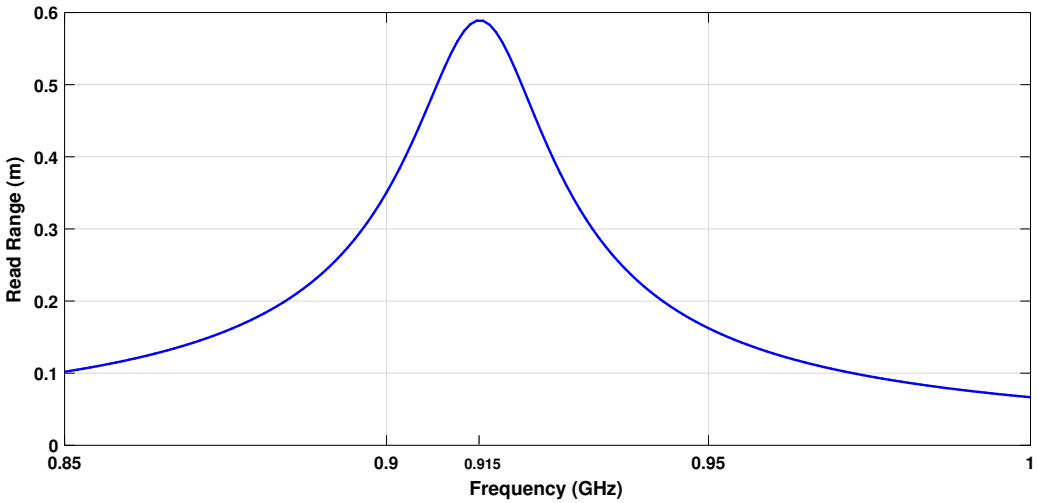

Figure 3.5: Read range for the optimized tag antenna attached on flat metallic object of 125 x 125 mm^2.

For estimating the radiation efficiency of the tag antenna, the induced current density is analyzed. The radiation efficient corresponds to the product of the efficiency of conduction and dielectric material in the antenna. To analyze this electromagnetic behavior, it is important to observe the amplitude of the surface current, which is concentrated on the

flat surface. Figure **3.6** shows the surface current density on copper plate with different sizes.

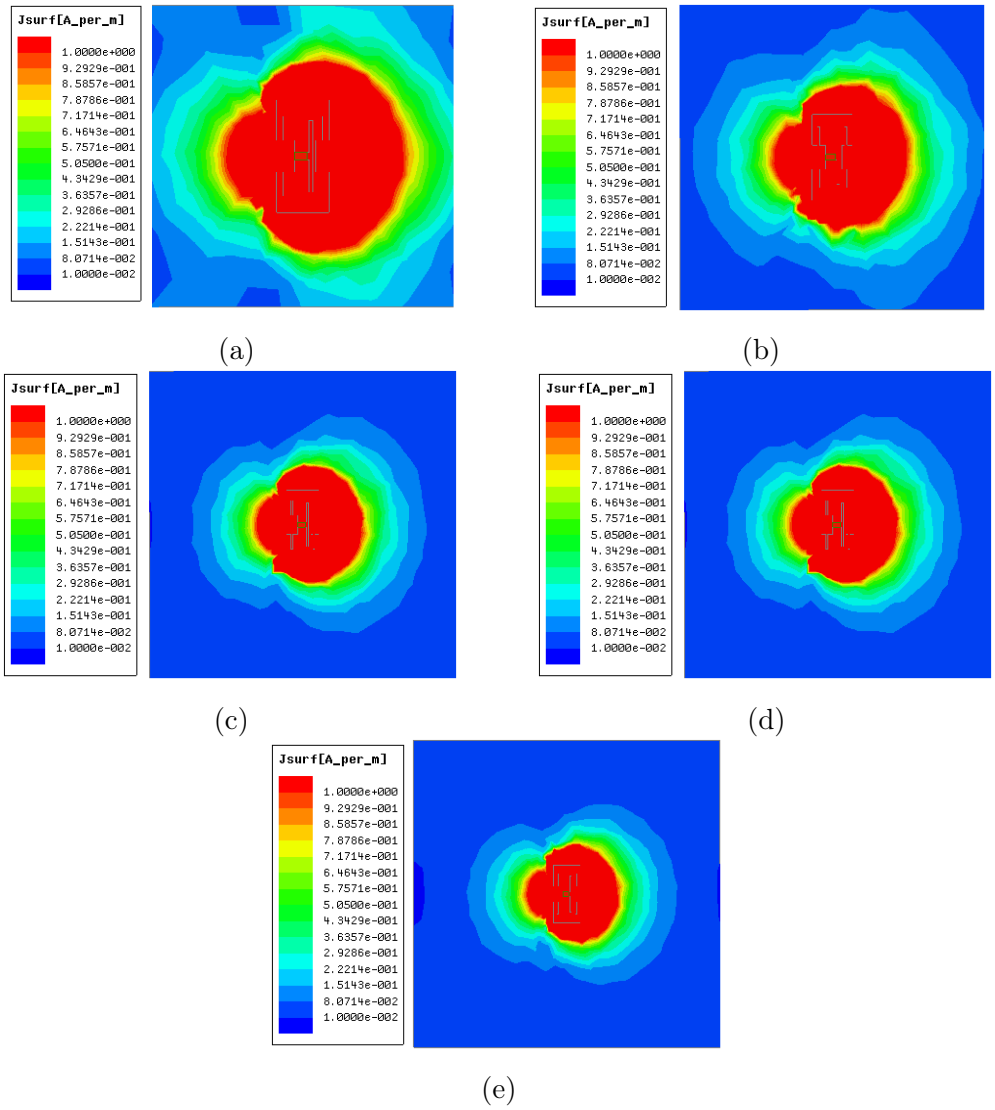

Figure 3.6: Current distribution for copper plate of: (a) 75 x 75 x mm^2, (b)100 x 100 mm^2, (c)125 x 125 mm^2, (d)150 x 150 mm^2, (e) 175 x 175 mm^2

Based on the results obtained on the current density on metallic plates, when the area of the copper plate increases, there is a higher separation of the currents stored on the edges of the metallic plate from the tag antenna. This is due to the decrease of diffractive events on the edges. In other words, the fringing fields at the antenna's edges can be suppressed.

Table **3.2** and Figure **3.7** show the antenna performance on different metallic surfaces. The performance of the RFID tag on a copper plate with square length of 125 mm and 150 mm improves slightly in comparison with other dimensions because of impedance matching at

915 MHz, achieving larger read range. Furthermore, the resonance frequency of the antenna increases mildly with the increment of the dimension of copper plate and the antenna gain keeps stable for all cases regardless of the square dimension.

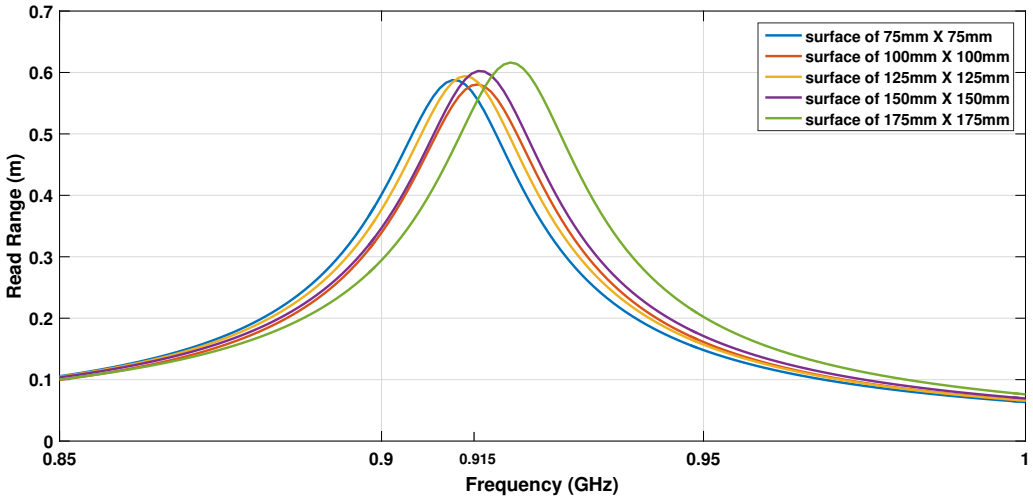

Figure 3.7: Read range of the tag antenna over copper plates with different dimensions.

Table 3.2: Simulated results of the tag antenna wrapped over copper plates with different dimensions at 915 MHz.

Parameter	**Square length**				
	75mm	**100mm**	**125mm**	**150mm**	**175mm**
Transmission coefficient	0.84	0.92	0.91	0.92	0.73
Gain (dB)	-26.71	-26.72	-26.64	-26.38	-26.09
Read range (m)	0.55	0.58	0.58	0.60	0.56

3.2.2. Antenna performance on copper cylinder

The antenna impedance for a cylinder metallic surface of radius=20 mm is depicted in Figures **3.8** and **3.9**. The antenna impedance at 915 MHz band is 6.8+267j Ω, which it represents a transmission coefficient of 0.23, value that is very limited and it hinders the proper backscattering process of the tag to reflect the incident power supplier by the reader. Therefore,

the return loss is about -1.11 dB at 915 MHz, as shown in Figure **3.10**, representing a poor impedance matching between the antenna and chip. The bandwidth of the tag antenna is about 7 MHz and it is covers the 904 MHz – 911 MHz frequency band.

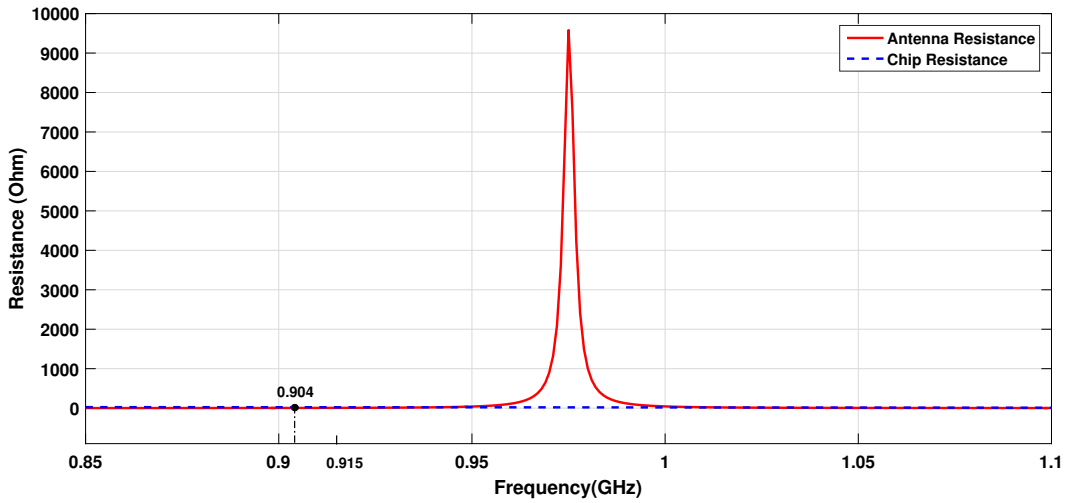

Figure 3.8: Resistance of the optimized tag antenna over a copper cylinder of radius=20 mm. The chip resistance is also shown.

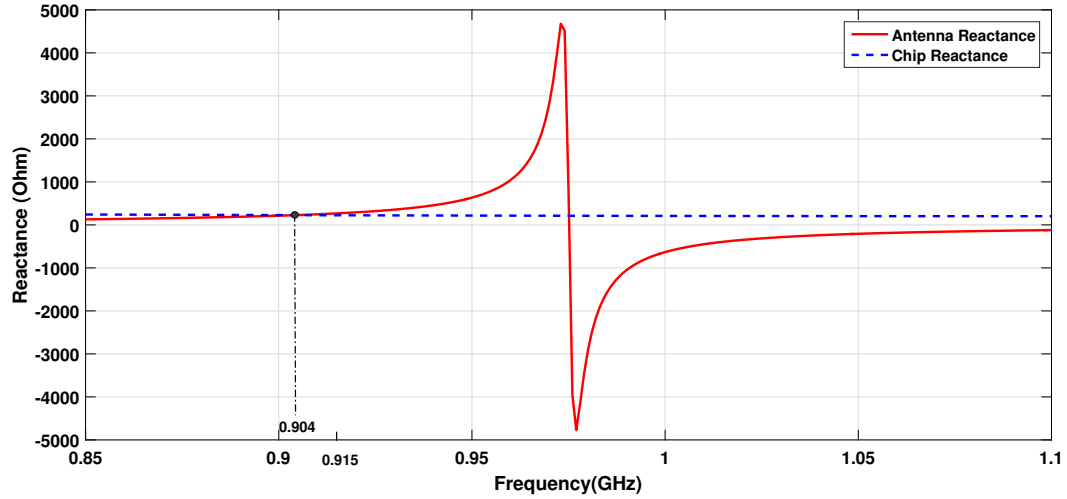

Figure 3.9: Reactance of the optimized tag antenna over a copper cylinder of radius=20 mm. The conjugate reactance of the chip is also shown.

Additionally, the poor impedance matching proves that to optimize the antenna on planar surfaces, when really is required to analyze its behavior on curved surfaces, is not a good

methodology because the optimization process would not be helpful in maximizing the antenna read range in the desired frequency.

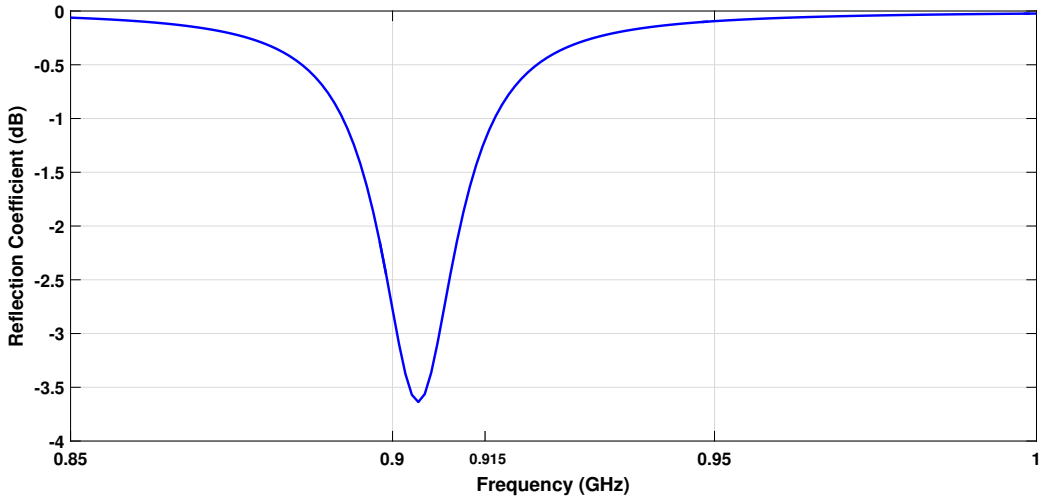

Figure 3.10: Power reflection coefficient for the tag antenna attached on copper cylinder of radius=20 mm.

On the other hand, Figure **3.11** displays the antenna gain, in the XZ plane and YZ plane, when it is mounted on copper cylinder of radius=20 mm. As it is possible to see, the gain is about -13.34 dB in the perpendicular axis of the tag antenna, value higher than that obtained on the copper plate. It also represents a maximum directivity of 4.94.

The radiation pattern presents a low front to back ratio, which is very important in RFID systems, because the coverage range of the tag antenna may be broader, and its radiation pattern may become more omni directional. Moreover, when the curvature of the antenna is high, the effective area enhances since the antenna manages to be more omni directional and the front-back relation tends to reduce.

Thus, the tag antenna can receive a better amount of power supplied for the reader in broader angles of reception. In such a way, the read range of the tag is 1.34 m at the frequency of 915 MHz when it is mounted on copper cylinders with radius=20 mm, like is depicted in Figure **3.12**.

Moreover, to estimate the radiation efficiency of the tag antenna mounted on metallic cylinders, it is very important to study the behavior of the current density for different radii and to analyze which electromagnetic effect occurs. Figure **3.13** illustrates the surface current density on copper cylinder with different radii. It is possible to see that the current

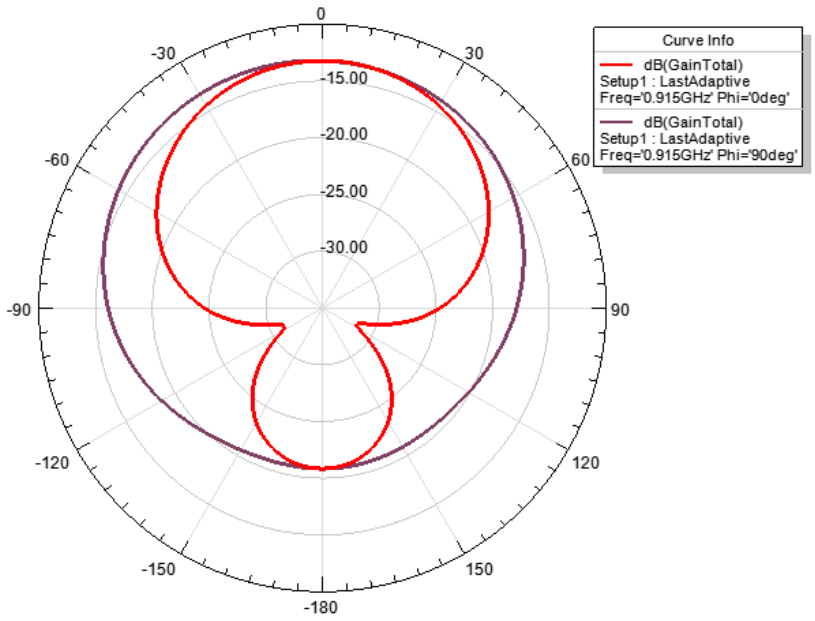

Figure 3.11: Gain of the proposed tag antenna on cylindrical metallic object with radius=20 mm in the XZ plane (ϕ=0°) and YZ plane (ϕ=90°) using genetic algorithm.

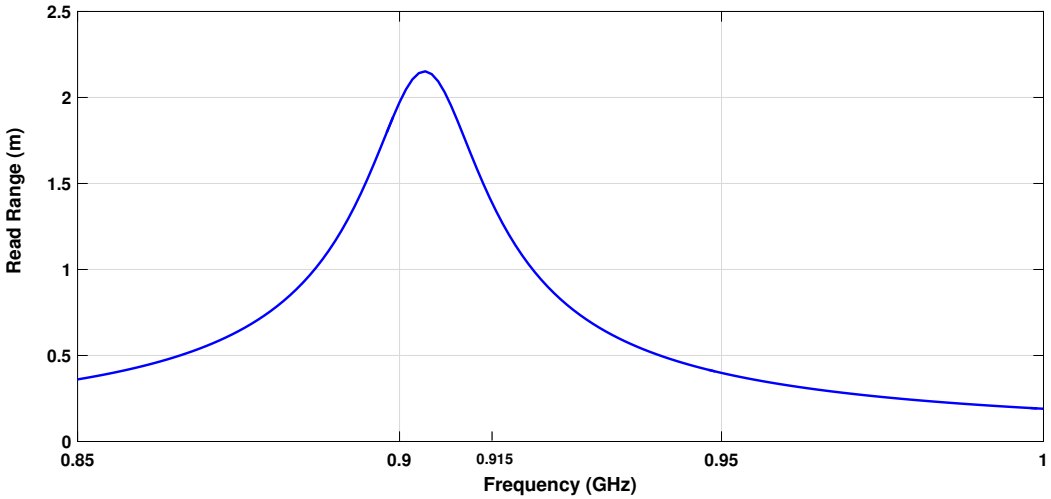

Figure 3.12: Read range for the tag antenna attached on copper cylinder of radius=20 mm.

density on the surface is distributed horizontally, in function of cylinder curvature. Also, the current density is stronger for cylinders with low radius, leading to efficiency to be increased.

As was previously analyzed in the section 2.5, the antenna curvature causes the reduction of

electric field and dissipation power in the antenna. Therefore, the antenna gain is enhanced with an increase of the curvature angle, as shown in Table **3.3**.

Table **3.3** and Figure **3.14** illustrate the main electromagnetic properties of the tag antenna on metallic cylinders with different radii. The resonance frequency of the small antenna decreases with the increase of the curvature. Then, the performance of the curved antenna keeps the studied hypothesis of cavity model.

Furthermore, the tag antenna has a limited transmission capability which does not surpass the 50 % of the incident power. This is produced by the difficulties to accomplish the impedance matching in the tag, when the antenna is bended.

Table 3.3: Simulated results of the tag antenna wrapped over cylindrical metallic objects with different radii at 915 MHz.

Parameter	**15mm**	**20mm**	**25mm**	**30mm**	**35mm**	**40mm**
Transmission Coefficient	0.16	0.23	0.26	0.28	0.30	0.45
Gain (dB)	-11.66	-13.34	-14.77	-15.70	-16.66	-17.62
Read Range (m)	1.35	1.34	1.20	1.14	1.11	1.16

Moreover, doing a comparative analysis between the results obtained from the antenna performance on both volumes, it is possible to affirm that the power transfer decreases 75 % when the antenna is attached to the cylinder with radius=20 mm than when it is on a flat object of 125 mm x 125 mm. Taking about the difference of read ranges for both volumes, it is possible to affirm that the planar surface presents a decrease of 57 % when compared to the metallic cylinder.

In the same way, in the next section, the results of the antenna optimization mounted directly on a copper cylinder is presented. The optimization based on a genetic algorithm is used, with the aim to compare the electromagnetic behavior of the optimization in both geometries and for creating an ideal methodology for the antenna design.

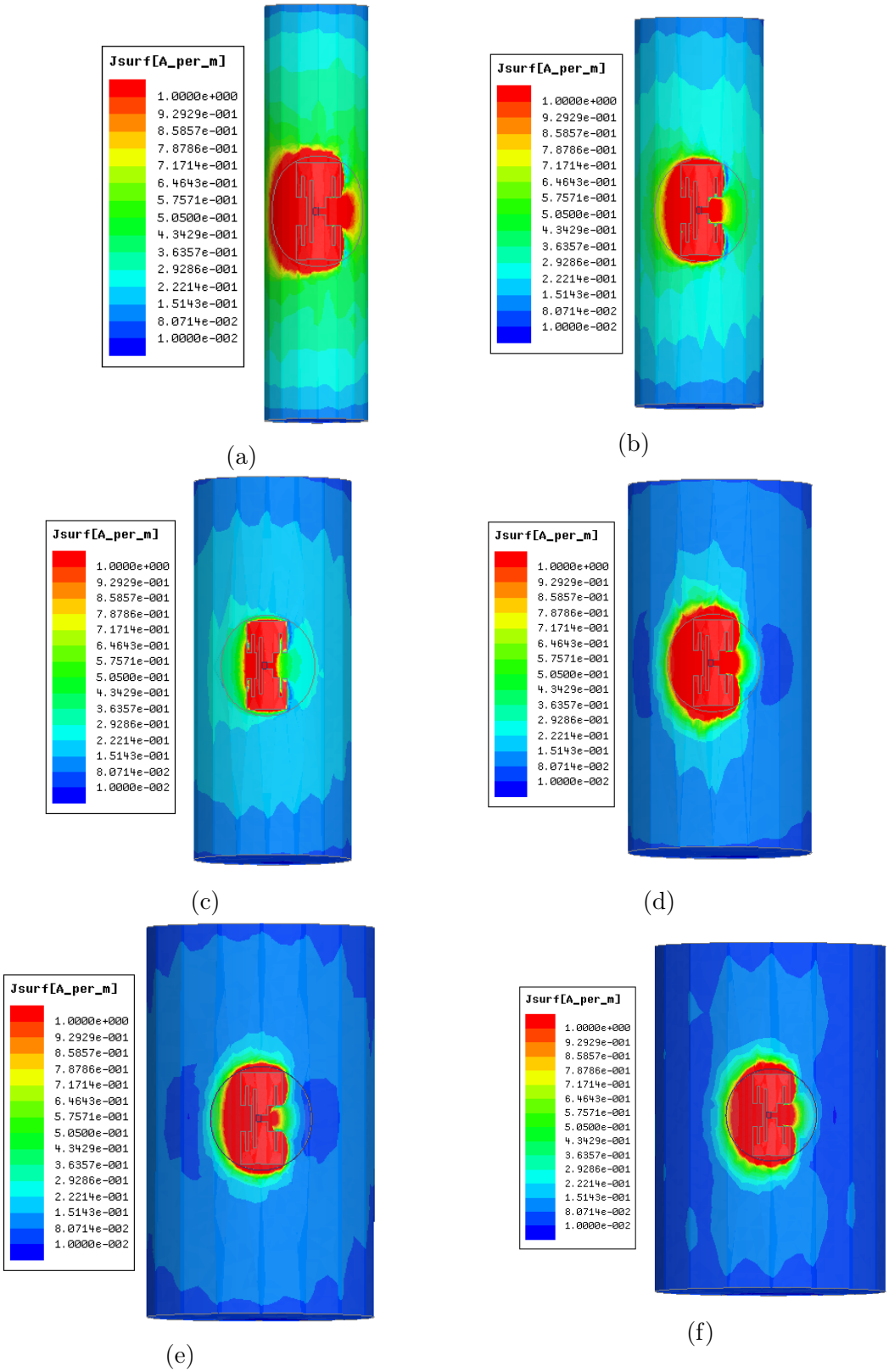

Figure 3.13: Current distribution for copper plate of height of 120 mm and radius of: (a)15 mm, (b)20 mm, (c)25 mm, (d)30 mm, (e)35 mm, (f)40 mm

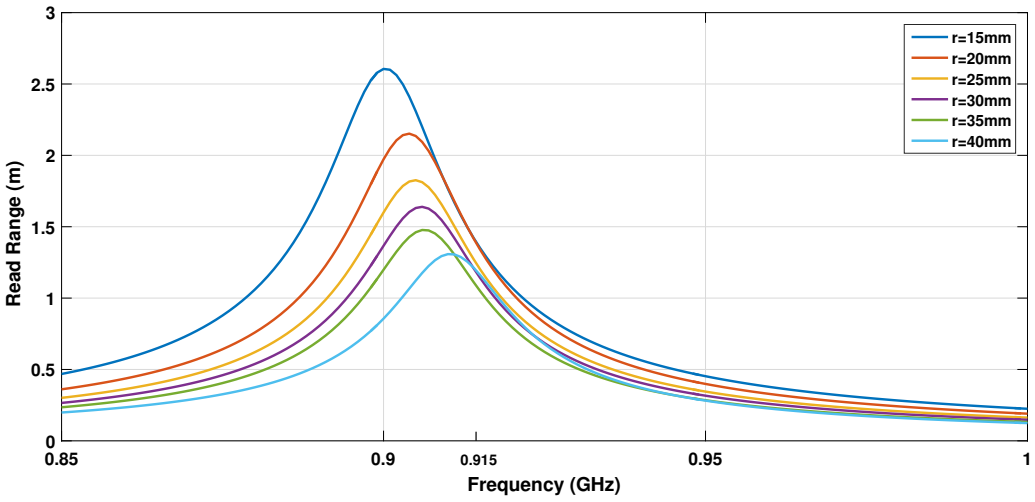

Figure 3.14: Read range of the tag antenna over cylindrical metallic objects with different radii.

3.3. Optimization on copper cylinder

In this section a new optimization was developed, using a genetic algorithm, for the tag antenna mounted directly on a copper cylinder with radius of 20 mm, with the aim of comparing the results obtained with to previous optimization done on the copper plate. Figure **3.15** shows the convergence results of the genetic algorithm for the evaluated objective function. It is possible to observe that the algorithm converges with 10 generations and a population of 25 individuals for each one. As expected, the last generation presents the best fitness value, achieving maximum read range of the tag antenna.

Based on the results obtained with the genetic algorithm, the following antenna parameters were defined in order to maximize the read range of the tag antenna for the metallic cylinder of radius=20mm. Table **3.4** exhibits the parameters of the optimized antenna using genetic algorithm.

Figures **3.16** and **3.17** shows the input impedance of the tag antenna on copper cylinder with a radius of 20 mm. For the desired frequency of 915 MHz, the antenna has an impedance of around 5.3+227j Ω, which promotes the complex impedance matching. In this case, it is very difficult to achieve a total complex matching due to the curved geometry of the metallic surface and the antenna bending effect. Then, the real impedance of the antenna differs from the chip resistance. The tag has a transmission coefficient of 0.57 on this surface, which represents a return loss of -3.7 dB, as depicted in Figure **3.18**.

Despite only 57 % of power being transferred to the antenna for the backscattering process

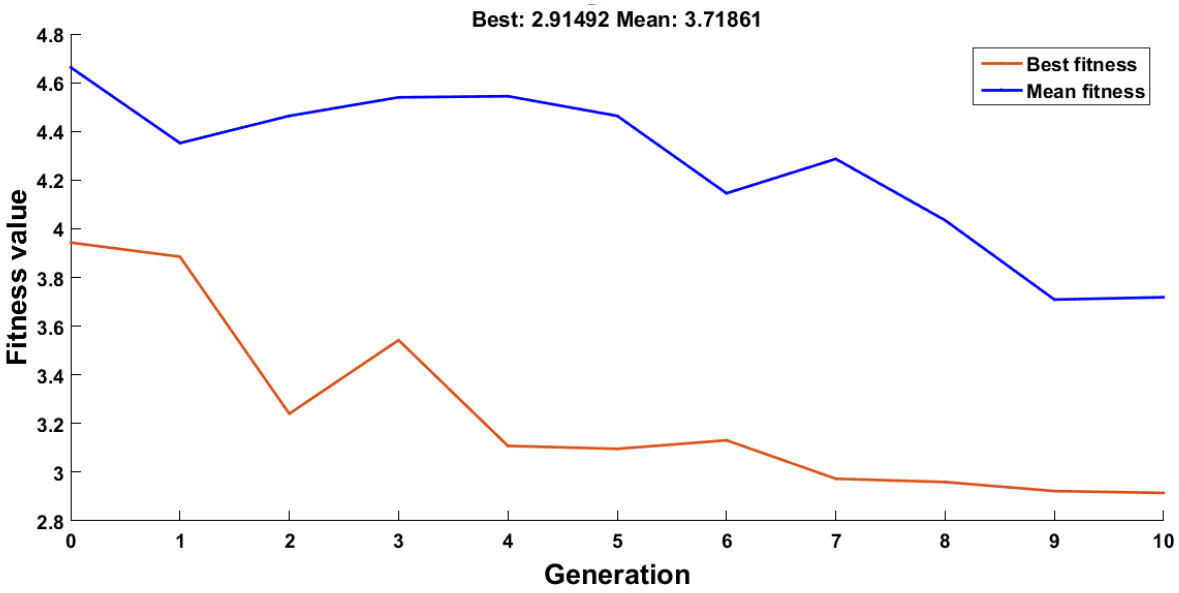

Figure 3.15: Fitness value of the genetic algorithm used to optimization procedure for a copper cylinder with radius=20 mm.

Table 3.4: Parameters and dimension of the tag antenna mounted on a copper cylinder using genetic algorithm

Parameter	**Length (mm)**	**Parameter**	**Length (mm)**	**Parameter**	**Length (mm)**
a	3.27	f	8.3	n	0.88
b	2	g	6.6	o	9.85
c	1.2	h	0.4	p	16.8
d	2	i	1	L	28
e	0.65	m	1.5	W	13

at 915 MHz, the bandwidth is about 8 MHz and it covers the 910 MHz – 918 MHz frequency band.

Figure **3.19** shows the radiation patterns of the tag antenna over a metallic cylinder with radius=20mm placed in Y-axis. First, the 2D radiation pattern for ϕ=0° and ϕ=90° is illustrated; and afterward, the 3D antenna pattern is depicted. The graphics illustrate the antenna gain, which on the perpendicular axis, presents a main lobule with a maximum gain of -13.37 dB.

The effective area of the antenna is broader with an increase of the antenna curvature. The-

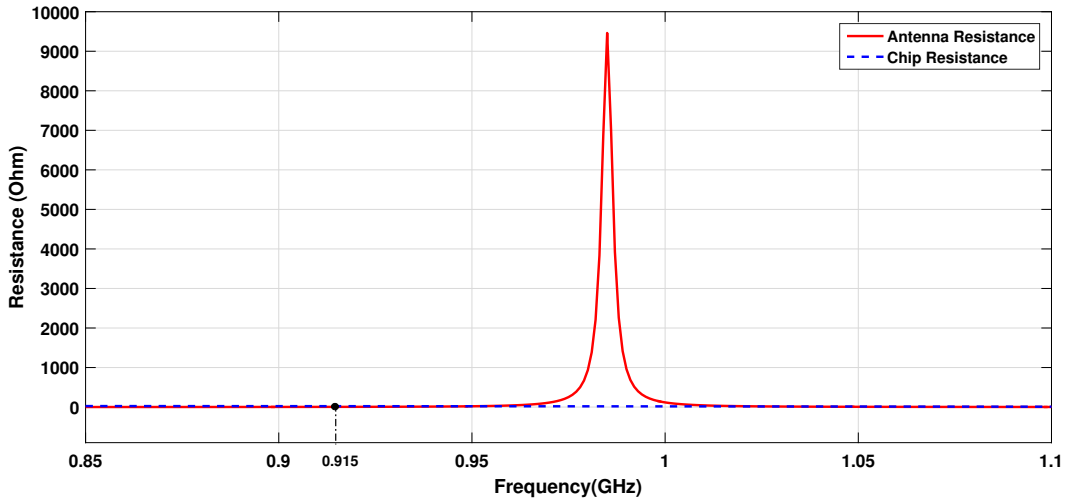

Figure 3.16: Resistance of the optimized tag antenna over a copper cylinder of radius=20 mm. The chip resistance is also shown.

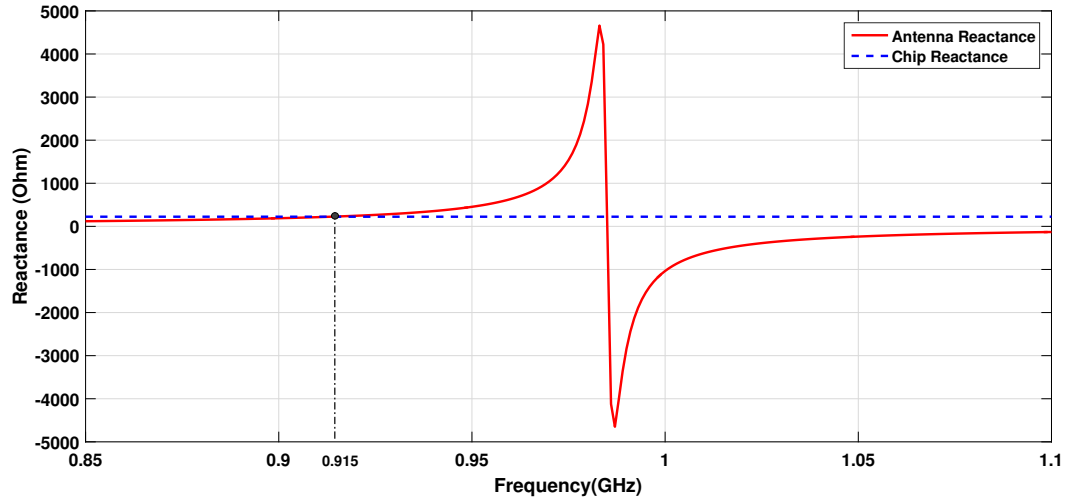

Figure 3.17: Reactance of the optimized tag antenna over a copper cylinder of radius=20 mm. The conjugate reactance of the chip is also shown.

reby, the radiation pattern presents a secondary lobule that improves the coverage area of the tag, and generates a comparable front-back ratio. This behavior tends to be more noticeable when the antenna bending effect is higher. Also, the maximum antenna directivity is 4.97 dB at 915 MHz, a larger value for this kind of geometries in comparison to metallic plates.

Figure **3.20** illustrates the read range of the optimized tag antenna on a metallic cylinder with radius=20 mm. Based on the graphic, the maximum distance between the reader

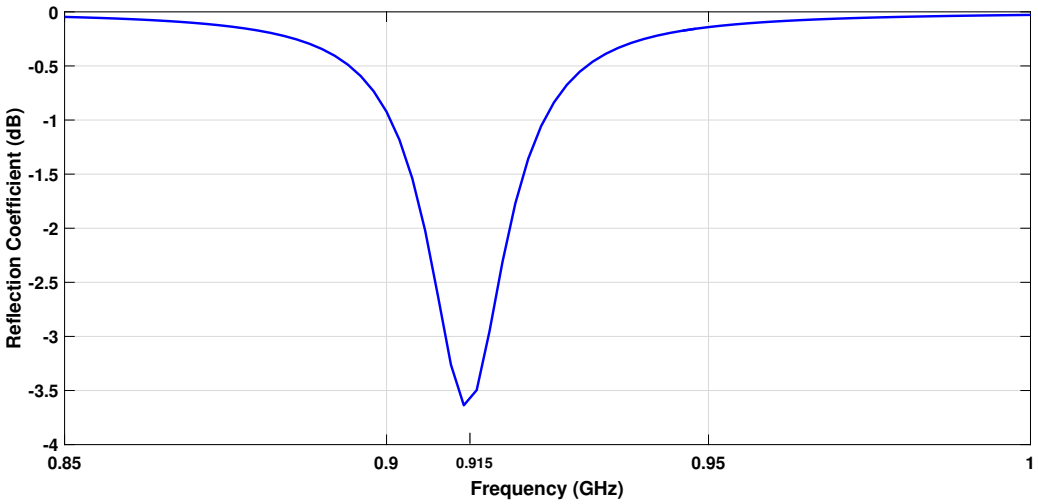

Figure 3.18: Power reflection coefficient for the optimized tag antenna attached on copper cylinder of radius=20 mm.

and the tag is 2.13 m at 915 MHz, important value for tracking of cylindrical metallic objects.

Figures **3.21** and **3.22** illustrate the electrical behavior of the antenna in terms of directivity, radiation efficiency and gain, with a variation of radius of the cylinder. The antenna directivity decreases with an increment of the curvature, due to part of radiated energy in the back side of the antenna. Moreover, its radiation efficiency increases, and therefore, the antenna gain improves. These results respect the hypothesis of the cavity model for curved antennas.

Table **3.5** and Figure **3.23** show the transmission coefficient, gain and read range of the optimized tag antenna on cylindrical metallic objects with different radii. According to the results, the resonance frequency of the tag antenna decreases for an increment of the antenna curvature. Also, the read range increases with the antenna curvature, improving the tag performance.

Additionally, an evaluation of the antenna performance on a copper cylinder with radius=80 mm was done. It was observed that the antenna read range decreases considerably to 0.63 m at 915 MHz, range of similar value as the copper plate with 125 mm x 125 mm. This proves how the antenna curvature affects the antenna performance.

Subsequently, a new optimization was done, using the genetic algorithm for the antenna mounted on cylinder copper of radius=40 mm. The optimized antenna achieved a read range about 1.3 m at 915 MHz. Despite maximizing the antenna read range on cylinders with

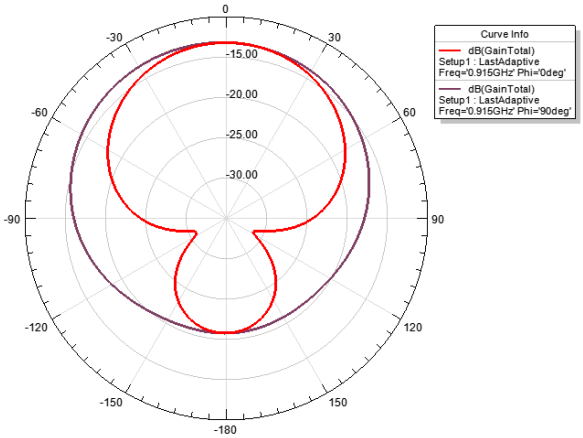

(a)

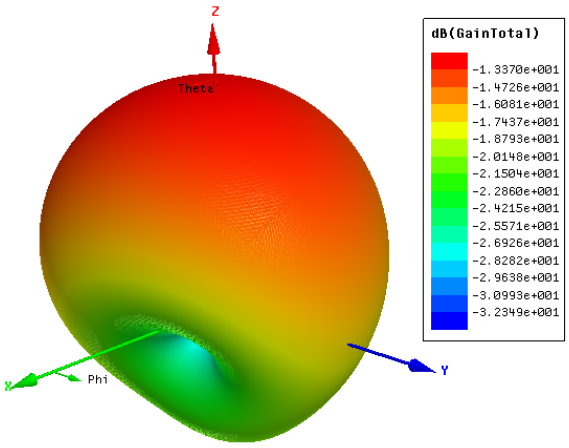

(b)

Figure 3.19: 2D and 3D radiation pattern of the tag antenna over metallic cylinder with radius=20 mm.

Table 3.5: Simulated results of the tag antenna wrapped over cylindrical metallic objects with different radii at 915 MHZ.

Parameter	**15mm**	**20mm**	**25mm**	**30mm**	**35mm**	**40mm**
Transmission Coefficient	0.54	0.57	0.54	0.56	0.54	0.54
Gain (dB)	-11.68	-13.37	-14.84	-15.84	-16.85	-17.63
Read Range (m)	2.51	2.13	1.75	1.58	1.38	1.27

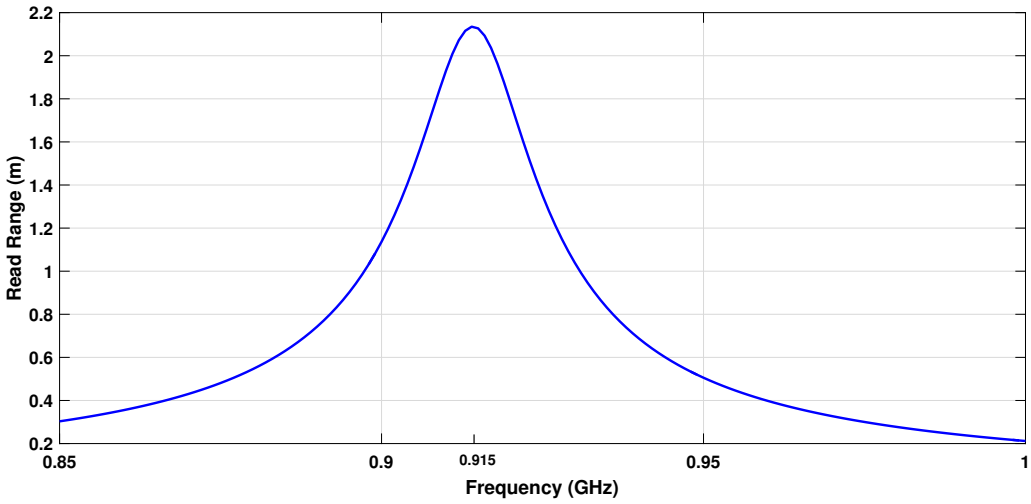

Figure 3.20: Read range of the optimized tag antenna attached on metallic cylinder with radius=20 mm.

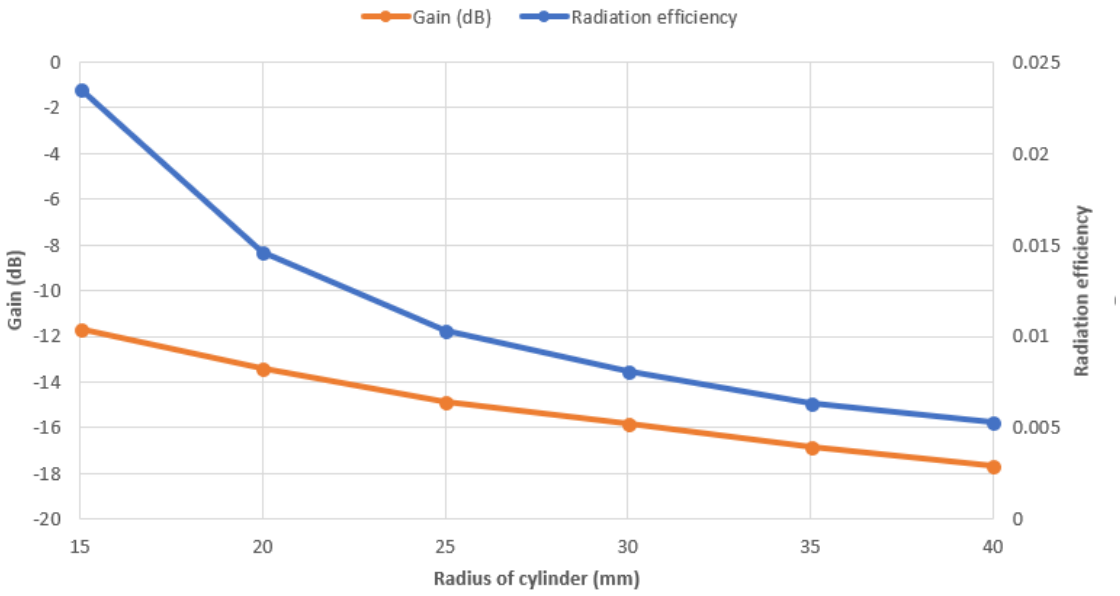

Figure 3.21: Transmission efficiency and gain of the tag antenna over cylindrical metallic objects with different radii.

higher radii, the antenna tends to decrease its curvature and behaving more similar to a planar surface, decreasing its read range.

On the other hand, for maximizing the antenna read range, it is important to consider not only a good impedance matching; the antenna gain also plays an essential role, as was seen in chapter 2. Figure **3.24** illustrates the read range variations of the dipole antenna for the

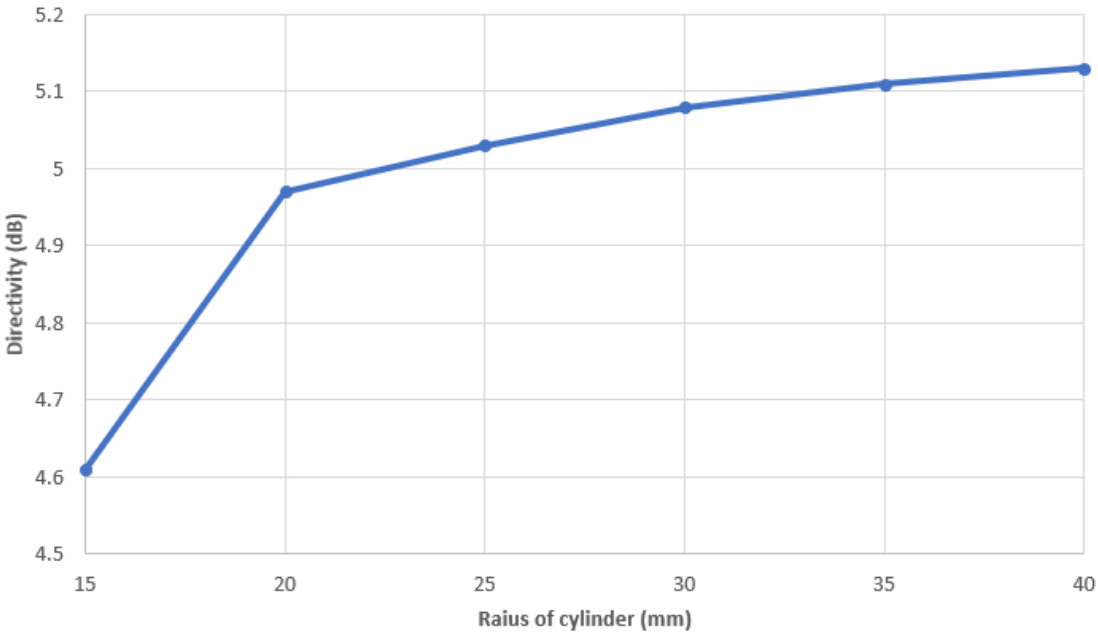

Figure 3.22: Directivity of the tag antenna over cylindrical metallic objects with different radii

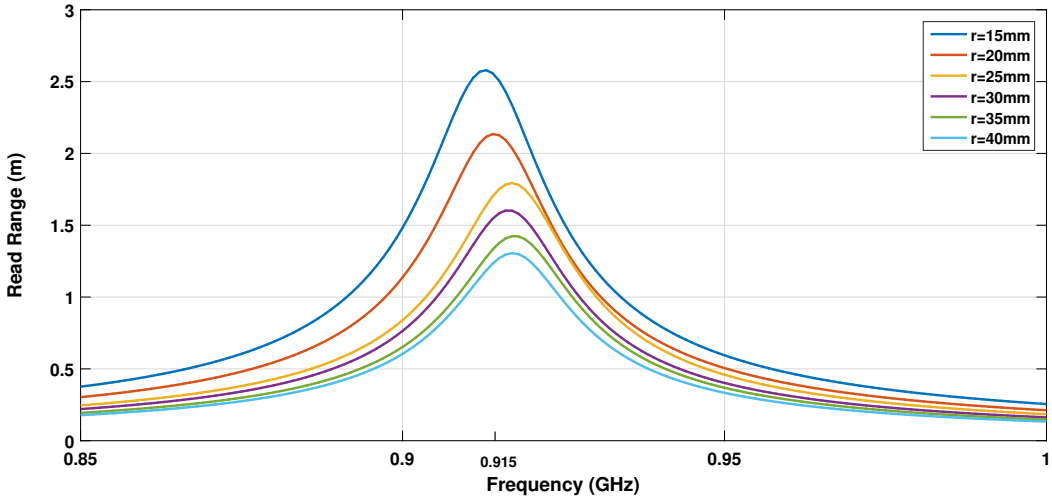

Figure 3.23: Read range of the tag antenna over cylindrical metallic objects with different radii.

three cases analyzed: an antenna 1 (results of the section 3.2.1), an antenna 2 (results of the section 3.2.2) and an antenna 3 (results of the section 3.3). According to the graph, tags mounted on a cylindrical surface, characterized for its high gain and limited impedance matching, have a better read range than tags attached on a flat surface, with characteristics of low gain and high impedance matching. Moreover, using the optimization directly on the

surface to be labeled (antenna 3) represents the best methodology to obtain a maximum coverage and a high antenna performance.

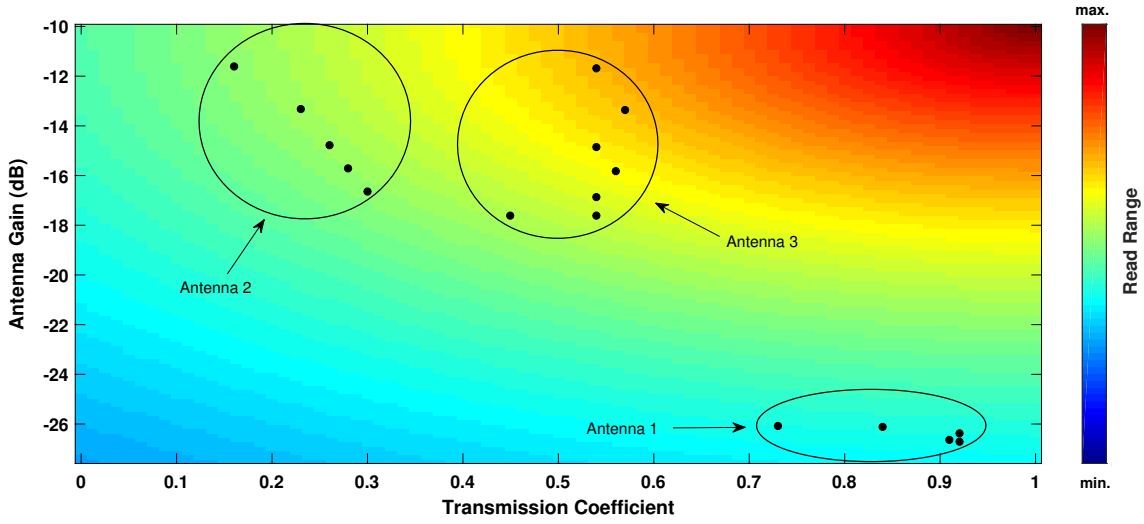

Figure 3.24: Variation of read range in function of power transmission coefficient and gain. The red color represents a maximum read range and the blue color a minimum coverage.

3.4. Optimization on PET cylinder

To analyze the electromagnetic behavior of the tag antenna on different kind of materials is an important challenge is to describe how the impedance matching between the tag antenna and the chip is affected. Therefore, achieving an antenna tuning in the desired frequency through optimization techniques is desirable. In this section, an analysis of the tag antenna on empty plastic cylinders and with liquid content is developed.

Tag antenna on empty PET cylinder

In this section, the simulated results obtained from the tag antenna mounted on plastic surface are shown, based on optimization procedure and an analysis of the antenna performance on cylinders with this kind of materials. It is important to highlight that all the analysis done in this research is applied to cylindrical surfaces with a height of 120 mm. Also, the cylinder surfaces were modeled using polyethylene terephthalate (PET) material with a dielectric constant of 2.8 and dielectric loss tangent of 0.003. The plastic thickness is 0.8 mm.

According to the results obtained through the antenna optimization using the genetic algorithm, in Table **3.6**, the following antenna parameters were established, ideally to maximize the read range of the tag antenna for the PET cylinder of radius=20 mm.

Table 3.6: Parameters and dimension of the tag antenna mounted on a PET cylinder using genetic algorithm.

Parameter	**Length (mm)**	**Parameter**	**Length (mm)**	**Parameter**	**Length (mm)**
a	3.3	f	8	n	0.8
b	2	g	6	o	10
c	1.2	h	0.4	p	17.5
d	2	i	1	L	28
e	0.7	m	1.5	W	13

The tag antenna has an impedance of 2.5+223.4j Ω at the central frequency of 915 MHz when it is mounted on an empty PET volume, as depicted in Figures **3.25** and **3.26**. For this case, despite the imaginary impedance being similar to the conjugated complex chip impedance, the total impedance matching is not ideal because the real impedances are different, therefore, the maximum power transfer between them is very limited. In the same way, the reflection coefficient is about -1.89 dB and the transmission coefficient is 0.35 at the desired frequency, which explain the poor total impedance matching between the chip and tag antenna.

The radiation pattern of the tag antenna on an empty plastic cylinder with radius=20 mm is shown on Figure **3.27**. The antenna gain is about -17.96 dB in its perpendicular axis and its radiation pattern presents a front-back ratio close to unity, value that is very important in RFID systems to provide broad coverage. Also, the antenna directivity on this plastic surface is 1.65 dB and its radiation efficiency is smaller than when antenna is wrapped on metallic cylinders.

Figure **3.28** illustrates the behavior of the radiation efficiency and antenna directivity when the tag is wrapped on PET cylinders with different radii. The antenna directivity improves with the increment of radius of the cylinder, due to the reduction of the radiated energy in the back side of the antenna.

Also, the antenna has a less directivity on plastic cylinder than for metallic cylinders as consequence of absorbent properties of PET (good dielectric), generating the antenna radiates

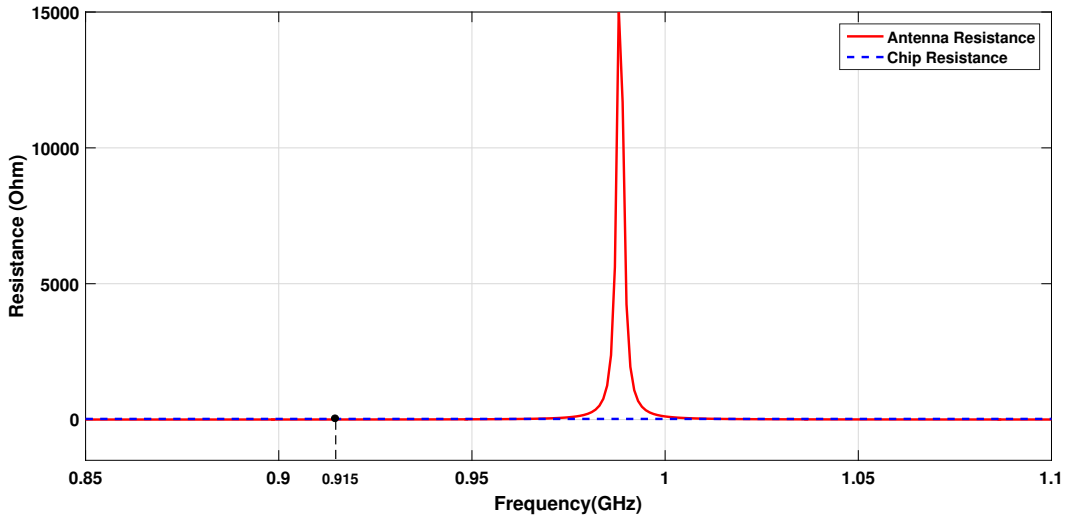

Figure 3.25: Resistance of the optimized tag antenna over a empty PET bottle of radius=20 mm. The chip resistance is also shown.

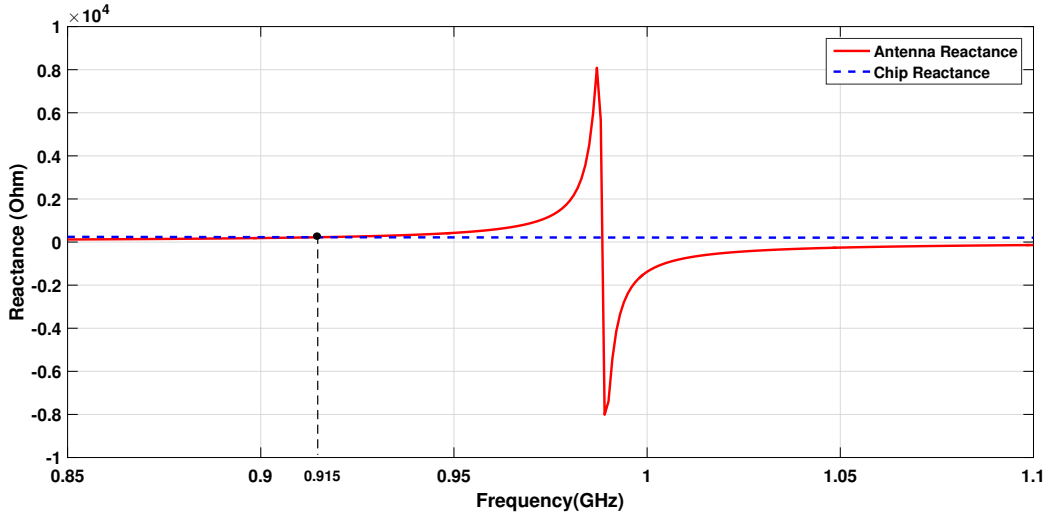

Figure 3.26: Reactance of the optimized tag antenna over a empty PET bottle of radius=20 mm. The conjugate reactance of the chip is also shown.

energy in both senses of its perpendicular axes, leading the front-back ratio can be close to unity. Consequently, the tag antenna can receive and reflect more energy supplied from to the reader signal on broader angles through the backscattering process.

On the other hand, the increase of the antenna curvature improves the radiation efficiency, producing the improvement of its gain. This electrical behavior responses satisfactorily the cavity model analyzed, inclusive for this type of materials.

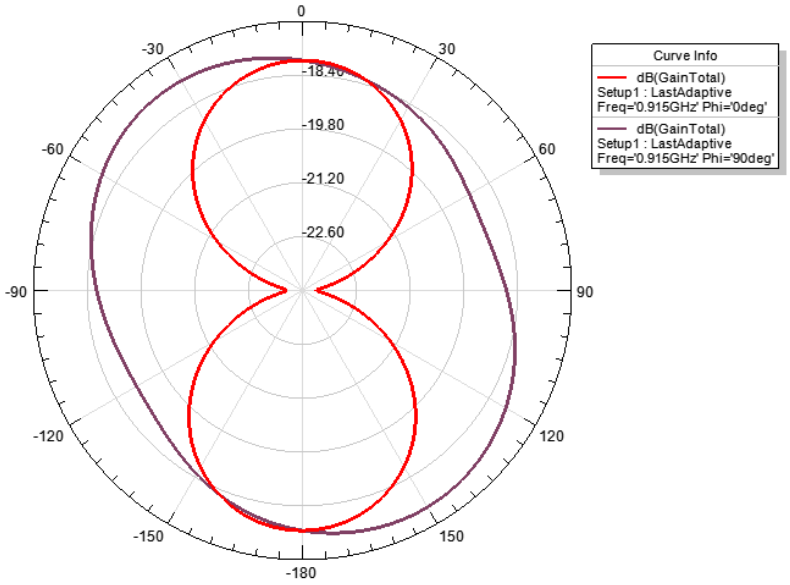

Figure 3.27: Gain of the proposed tag antenna on empty PET bottle with radius=20 mm in the XZ plane (ϕ=0°) and YZ plane (ϕ=90°).

In addition, the current density distribution on the PET cylinder keeps uniform for radii.

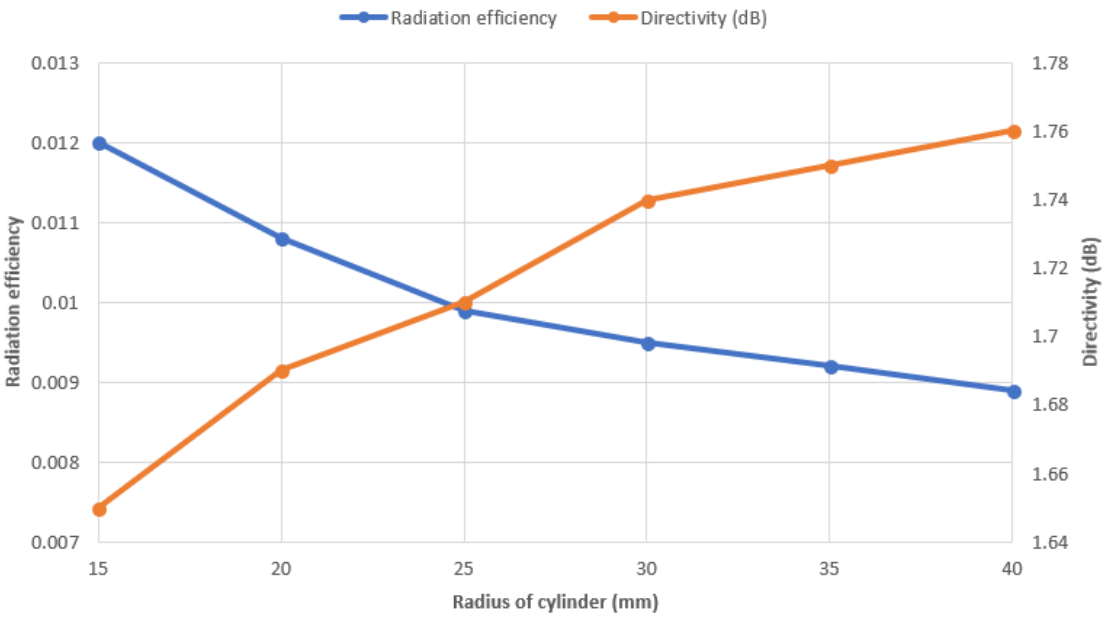

Figure 3.28: Directivity and radiation efficiency of the tag antenna over PET cylinder with different radii.

Figure **3.29** illustrates the read range reached by the tag antenna on plastic cylinder of radius=20 mm. It is possible to remark that the dipole antenna operates at the central frequency of 915 MHz with about 1 meter of coverage.

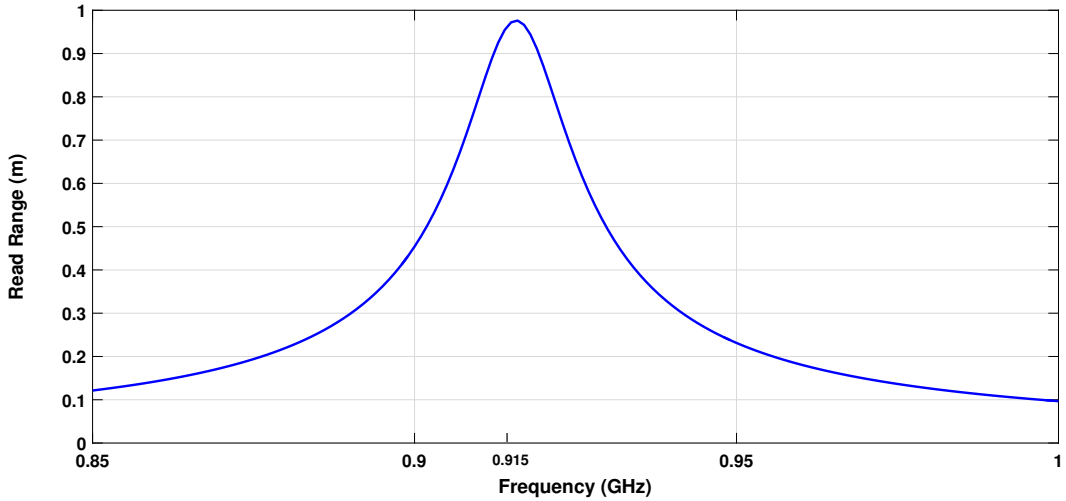

Figure 3.29: Read range of the tag antenna mounted on empty PET bottle with radius=20 mm.

Table **3.7** and Figure **3.30** show the gain and the read range of the tag antenna for different empty PET cylinders. The effect of the curvature on antenna performance produces a slight displacement in the operating frequency of the tag. The analysis of the cylindrical cavity model explained in section 2.5 and the results obtained indicate that the reduction of resonant frequency is due to the increase of the antenna curvature.

Table 3.7: Simulated results of the tag antenna on empty PET bottles with different radii at 915 MHz.

Parameter	**15mm**	**20mm**	**25mm**	**30mm**	**35mm**	**40mm**
Transmission Coefficient	0.29	0.35	0.34	0.30	0.30	0.32
Gain (dB)	-17.55	-17.96	-18.32	-18.46	-18.6	-18.73
Read Range (m)	0.93	0.98	0.92	0.85	0.84	0.86

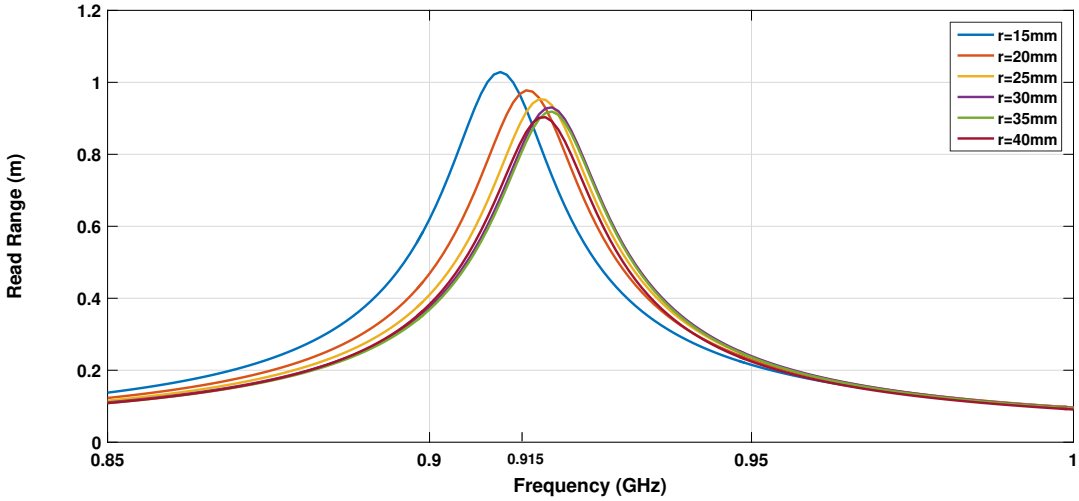

Figure 3.30: Read range of the tag antenna on empty PET bottles with different radii.

Tag antenna on PET cylinder with liquid contents

The RFID tag antenna presents a variation of its electromagnetic properties when different kind of liquids inside the plastic cylinders are added. Basically, this variation is produced by the adding a new dielectric with the PET volume, creating a multilayer dielectric with a higher effective permittivity.

Table **3.8** and Figure **3.31** show the influence of the liquid content in a plastic cylinder with radius=20 mm on the tag performance. The analysis was done for five liquids: water, glycerin, ethanol, acetone, and olive oil, which have a dielectric constant of 81, 47, 24.3, 20.7 and 3.1; and dielectric loss tangent of 0.157, 0.2, 0.25, 0.25 and 0.04, respectively. It is possible to observe that for all liquids, the tag antenna operates at the desired frequency band, around of 915 MHz. The displacement of the frequency is minimal due to the presence of ground plane behind of the substrate, which isolates the dielectric layers. Besides, the liquids with higher dielectric constants have a high antenna gain and read range.

The radiation efficiency of the tag antenna over a PET bottle with the presence of liquid content is limited because of the absorption of electromagnetic energy by the multilayer dielectric. Furthermore, the tag antenna on a PET bottle with liquid content can potentially increase the antenna impedance, improving its radiation efficiency [35].

Moreover, the PET bottle with a liquid of high permittivity, act as a conductor plane, reflecting the incident signals provided from the reader. Thus, the antenna directivity improves. In addition, as shown in equation (2.20), the dissipated power depends on the electric field provided by the antenna and the dielectric loss tangent of the liquid. Then, for low values

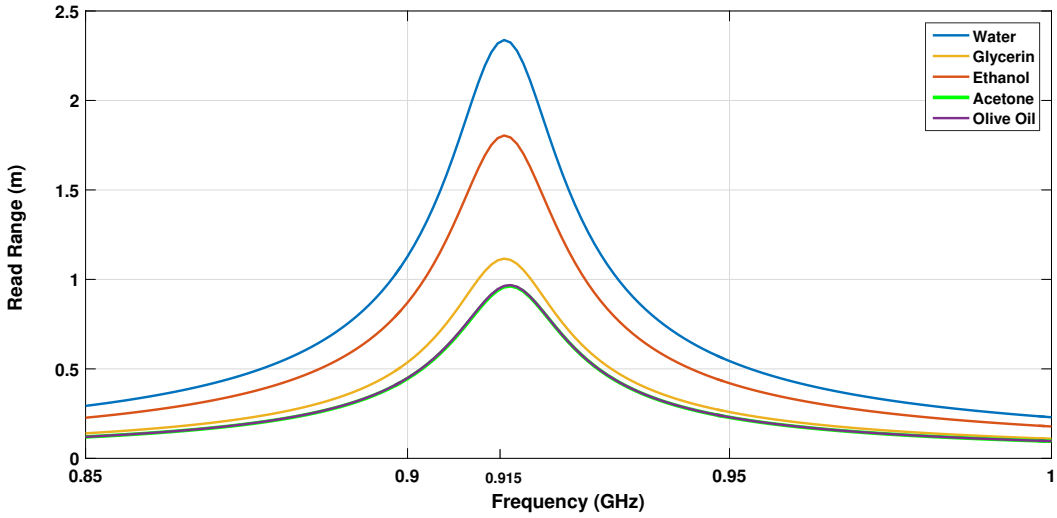

Figure 3.31: Read range of the tag antenna on PET bottle of radius=20 mm with different liquid contents.

Table 3.8: Simulated results of the tag antenna on PET bottle of radius=20 mm with different liquid contents at 915 MHz.

Parameter	**Water**	**Glycerin**	**Ethanol**	**Acetone**	**Oliver Oil**
Transmission Coefficient	0.36	0.36	0.35	0.34	0.40
Gain (dB)	-10.54	-12.76	-16.83	-17.98	-18.84
Read Range (m)	2.34	1.81	1.12	0.96	0.95

of permittivity, the PET bottle with the liquid absorb the incident energy, increasing the dissipated power, which leads to obtain a low radiation efficiency, as illustrated in Figure **3.32**. Furthermore, the current density distribution on the PET cylinder increases as the liquid permittivity rises.

However, for olive oil, liquid with the lowest permittivity, the radiation efficiency is higher than acetone and ethanol. It is due to its dielectric loss tangent, which is very low compared with the other liquids. Therefore, the PET bottle with olive oil allows the antenna can dissipate less energy than acetone and ethanol.

The high dielectric constant of water, for example, helps reducing the secondary lobules or nulls in the radiation pattern of the tag antenna [35]. For these reasons, the radiation pat-

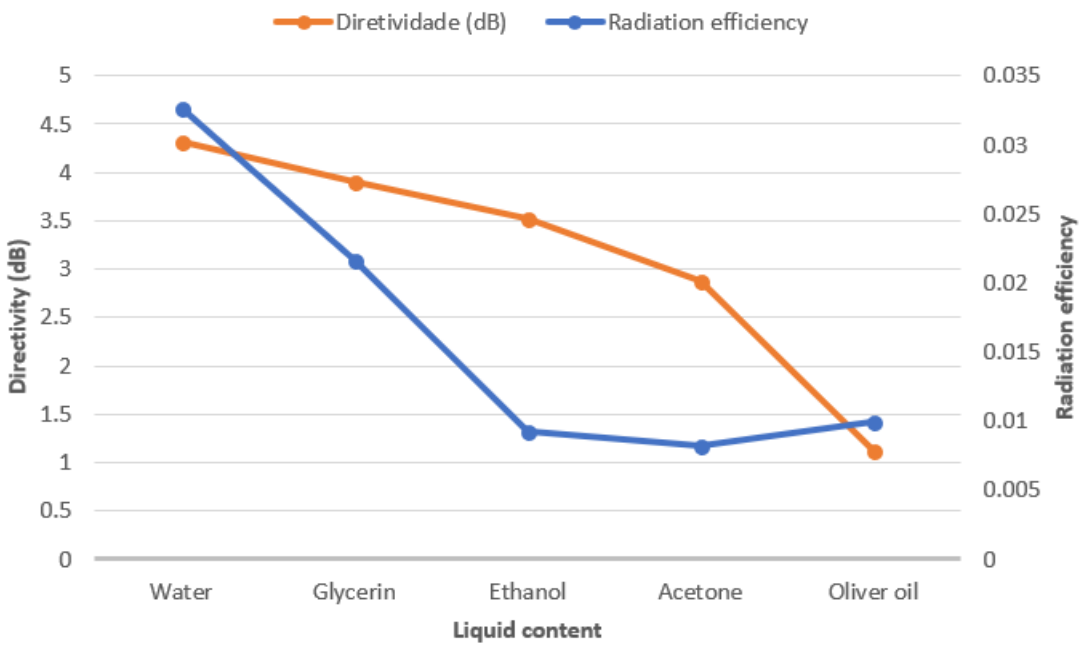

Figure 3.32: Directivity and radiation efficiency of the tag antenna over PET bottle of radius=20 mm with different liquid contents.

tern tends to be more directive and the read range of the tag enhances, when the dielectric constant of the liquid increases.

Moreover, the presence of ground plane behind of the substrate helps isolate the dielectric substrate and the dielectric multilayer. The ground plane inserted in the tag antenna acts as a reflector and it helps prevent any disturbance from the plastic surface [14, 19]. Moreover, the ground plane allows for good impedance matching between the chip and the tag antenna in the desired frequency. On the contrary, it could exist an antenna detuning for frequencies in the order of GHz.

3.5. Discussions

- The selected dipole antenna does not present a good performance on planar metallic objects since the read range is low. Therefore, the tag antenna performance is considered efficient and reliable only when it is wrapped on curved volumes, as consequence the effect of antenna bending which it improves the read range.

- According to the results obtained for the antenna optimization, using the genetic algorithm, for the copper plate of 125 mm x 125 mm, it is possible to cite that the antenna

performance wrapped on the metallic cylinder of radius=20 mm presents a higher read range of about 57 % in regard to the antenna mounted on the planar surface of 125 mm x 125 mm. This explains that the antenna curvature affects positively the antenna performance due to the significant increase in the antenna gain.

- Moreover, the use of the genetic algorithm directly on the copper cylinder allows that the antenna performance may be improved by about 37 % than the antenna optimization using the genetic algorithm on a flat surface, when the applicability of the RFID tag is for a copper cylinder with radius=20 mm.
- Figure **3.33** displays the antenna performance on empty plastic bottle and with different kind of liquids. As was analyzed previously, the dielectric constant of the liquid has an important influence on the antenna performance due to the increment of the antenna gain as consequence of the increase of the liquid permittivity.

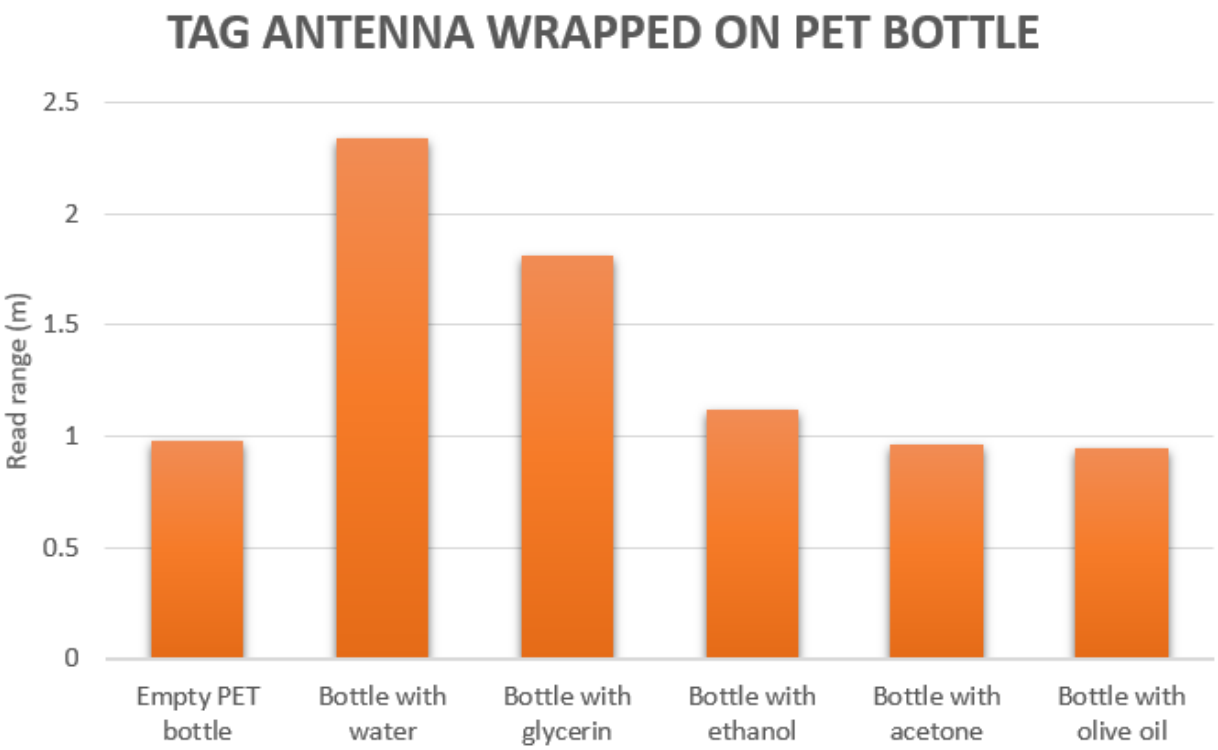

Figure 3.33: antenna performance on PET bottle with different kind of liquids.

4 Measurements

Generally, most tag antennas used for RFID applications are balanced. A dipole can be defined as a balanced antenna due to its symmetry and because it has current flowing on both legs. In this way, the dipole needs equal or balanced currents along its arms to operate properly, and then, the balanced antenna must be connected to a balanced feeder [36]. Another definition of balanced antenna is that a balanced antenna is a radiator which has neither conductor connected directly to the ground, and the impedance between ground and each conductor is the same. Also, a balanced line is a transmission line where the impedance between ground and each conductor is identical [37].

The impedance of the balanced antenna cannot be measured directly with devices that are terminated in unbalanced ports as coaxial ports. Coaxial cable is unbalanced due to the impedance between the ground and the outer conductor shield being different to the impedance between ground and the inner conductor [37]. The coaxial cable has a central conductor and an outer conductor, and they are not symmetrical. Therefore, when a unbalanced coaxial cable is connected to a balanced antenna, it is possible that the current flows on the outside of the outer conductor, affecting the radiation pattern [38].

4.1. Differential S-parameter method

A balanced dipole antenna can be represented by a two-port network, as shown in Figure **4.1**. The equivalent two-port network is used to determine the antenna impedance through the measurement of the S-parameters on the two feeding ports located on the both radiators of the dipole. The positive and negative ports of the source are connected to the input terminals of dipole arms, producing voltages V_1 and V_2 with a virtual ground plane. Also, the voltage difference on the two feeding ports is defined as V_d.

Figure **4.2** shows another representation of the two-port network from the point of view of the transfer function model and the mutual impedance equivalent circuit. Based on the T-network equivalent, the port voltages and currents are given by:

$$V_1 = Z_{11}I_1 + Z_{12}I_2 \tag{4.1}$$

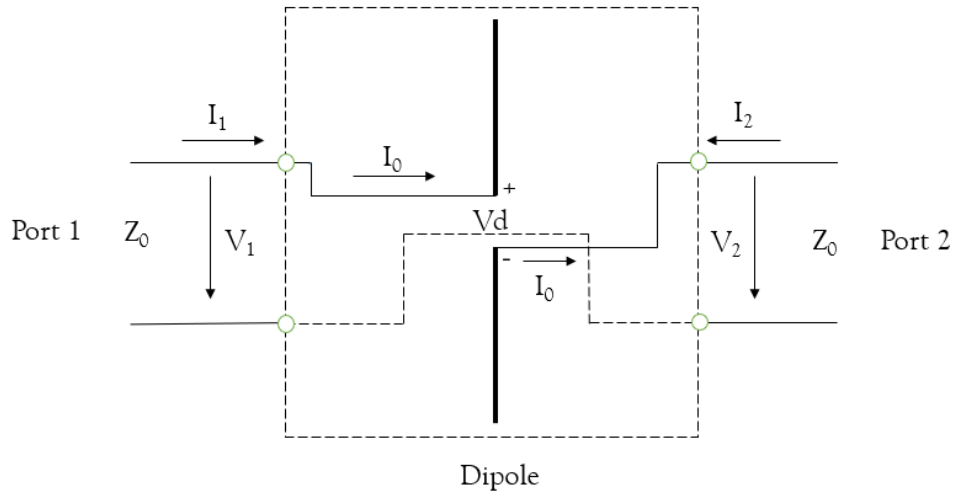

Figure 4.1: Two-port network representation of the dipole antenna.

$$V_2 = Z_{21}I_1 + Z_{22}I_2 \tag{4.2}$$

Considering I_1=I_0 and I_2=-I_0, the differential voltage V_d can be expressed as:

$$V_d = V_1 - V_2 = (Z_{11} - Z_{21} - Z_{12} + Z_{22})I_0 \tag{4.3}$$

Then, the impedance becomes:

$$Z_d = \frac{V_d}{I_0} = \frac{V_1 - V_2}{I_0} = Z_{11} - Z_{21} - Z_{12} + Z_{22} \tag{4.4}$$

Converting the Z-parameters to S-parameters and considering that Z'_d=$Z_0 Z_d$, the antenna impedance becomes:

$$Z'_d = \frac{2Z_0(1 - S_{11}S_{22} + S_{12}S_{21} - S_{12} - S_{21})}{(1 - S_{11})(1 - S_{22}) - S_{21}S_{12}} \tag{4.5}$$

Where Z_0 is the characteristic impedance of the coaxial cable, which is 50 Ω for the RG-58 coax used to execute the impedance measurements though the two ports of the Vectorial Network Analyzer (VNA). As a dipole antenna is balanced, then $S_{11} = S_{22}$ and $S_{12} = S_{21}$. Therefore, it is possible to simplify the equation (4.5) to:

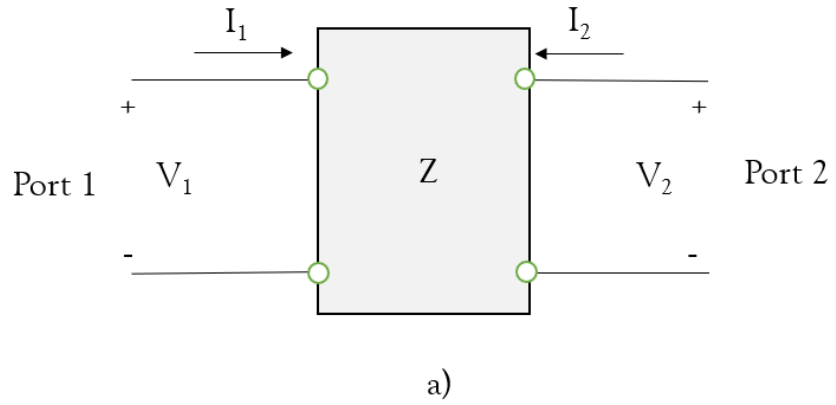

a)

(a)

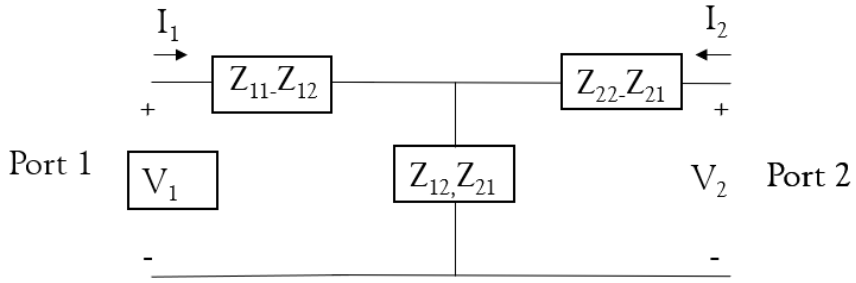

b)

(b)

Figure 4.2: (a) Two-port network and (b) T-network equivalent

$$Z'_d = \frac{2Z_0(1 - S_{11}^2 + S_{21}^2 - 2S_{21})}{(1 - S_{11})^2 - S_{21}^2} \tag{4.6}$$

4.2. Test fixture

The configuration of the balanced system to perform the measurements is illustrated in Figure **4.3**. The test fixture or also called jig, is a prototype formed by two semi-rigid coax cables whose outer conductors are joined together by a rolled tin as shown in Figure **4.4**. At the end of the prototype, the inner conductors are placed openly to be connected to the antenna feed points. On the other extremity of the fixture, a female SMA connectors are

placed, to made the connection to the network analyzer [39, 40] using test cables RG-58 50 Ω coax.

Therefore, the test fixture guarantees that the feed points of the balanced antenna may be driven by equal but opposite currents [41].

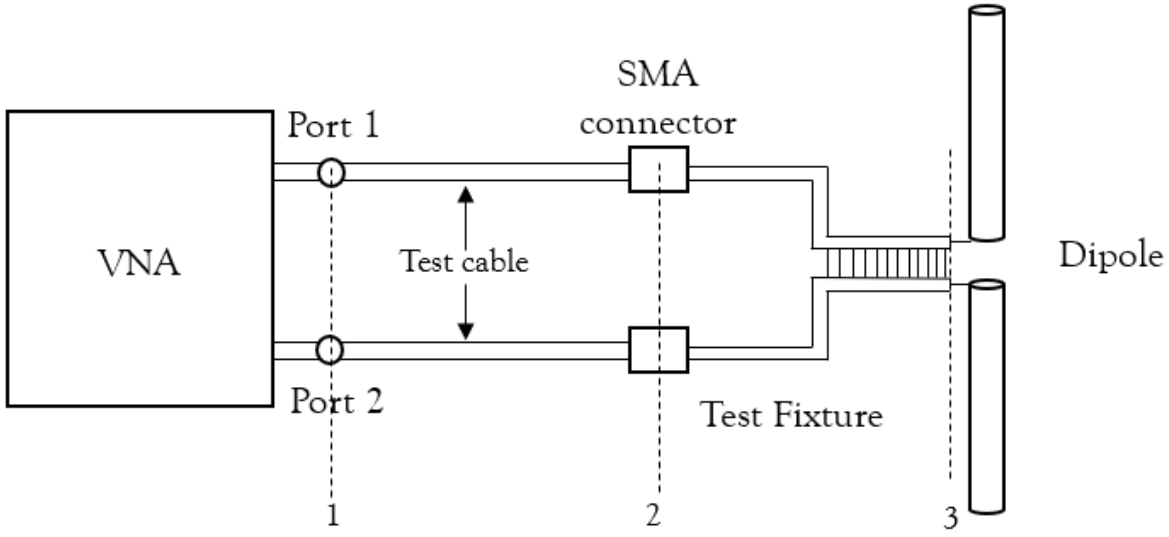

Figure 4.3: Configuration of the test fixture to measure the dipole impedance.

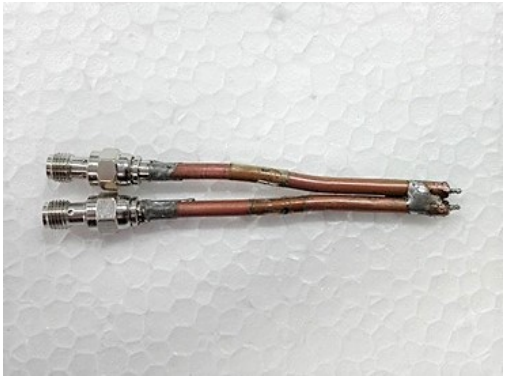

Figure 4.4: Test fixture used to develop the measurements.

4.3. Measurement process

The following steps were used to execute a proper measurement process of the balanced antenna:

a) Before to execute the measurements, it is suggested to prove the test cables which are connected to the test fixture and VNA. Then, it is necessary connecting the test cables to a 50 Ω load, and to observe how much power is reflected. A standard return loss (S_{11}) lower than -10 dB is acceptable, to assure a 90 % of the transmitted energy.

b) Developing a proper VNA calibration guarantees a good measured result, especially when working with microwaves frequencies because can exist some inaccuracies. For this project, a Rohde & Schwarz ZVL-6 Vector Network Analyzer [42] was used, with an operable bandwidth of 9 KHz to 6 GHz, resolution of 1 Hz, impedance of 50 Ω, and two ports to compute four S-parameters. Furthermore, to execute the calibration process, two calibration kits were used, with impedance of 50 Ω: 3.5 mm female Rohde & Schwarz ZV-Z135 model [43] and the N-type JBM-J2061 [44]. The calibration kits operate in the DC-15 GHz frequency band, and are used to correct the residual impedance of the system, to obtain accuracy results. It is very important to allude that for the second kit was added a N type – SMA adapter, to permit the connection of the calibration kit with the test cables.

The calibration process was carried out first, setting the operating bandwidth of the measurements. Secondly, the TOSM (Thru, Open, Short and Match) method was applied, which evaluates and calibrates the two ports of the VNA, using four standard configurations: Open, Short and Match for each port, and Thru standard between the two ports of the VNA. With this process, to shift the calibration plane of the VNA's connectors to the SMA connectors of the test fixture (from 1 to 2, see Figure **4.3**) is desirable, using the calibration kits, to compensate the effect of the test cables and connectors in the measurements [45].

c) Shifting the measurement plane to the tips of the fixture (from 2 to 3, see Figure **4.3**). The goal of this step is annulling the effects of the test fixture in the measurements. The shift of plane can be done in open or short circuit. Short circuited configuration requires welding the tips of the test fixture with the outer conductors of its coaxial cables (ground) [46]. In other words, welding the port 1 and ground (short1), port 2 with ground (short2), and short between two ports (short12). This configuration is recommended because the open condition is difficult to achieve for high frequencies [45].

d) Connecting the dipole antenna to the test fixture and execute the measurements of the S-parameter matrix. Figure **4.5** shows the configuration used to measure the tag antenna inside a anechoic chamber. The prototype built has the dimensions presented in Table **3.4**. Moreover, the measurements were developed on a copper cylinder with radius=20 mm.

e) Compensating the effect of the test fixture in the antenna measurements, applying the

following equations:

$$S_{11}^{corrected} = -\frac{S_{11}^{antenna}}{S_{11}^{short1}} \tag{4.7}$$

$$S_{12}^{corrected} = \frac{S_{12}^{antenna}}{S_{12}^{short12}} \tag{4.8}$$

$$S_{21}^{corrected} = \frac{S_{21}^{antenna}}{S_{21}^{short12}} \tag{4.9}$$

$$S_{22}^{corrected} = -\frac{S_{22}^{antenna}}{S_{22}^{short2}} \tag{4.10}$$

e) At last, to apply the differential S-parameter method analyzed in the section 4.1, for computing the antenna impedance.

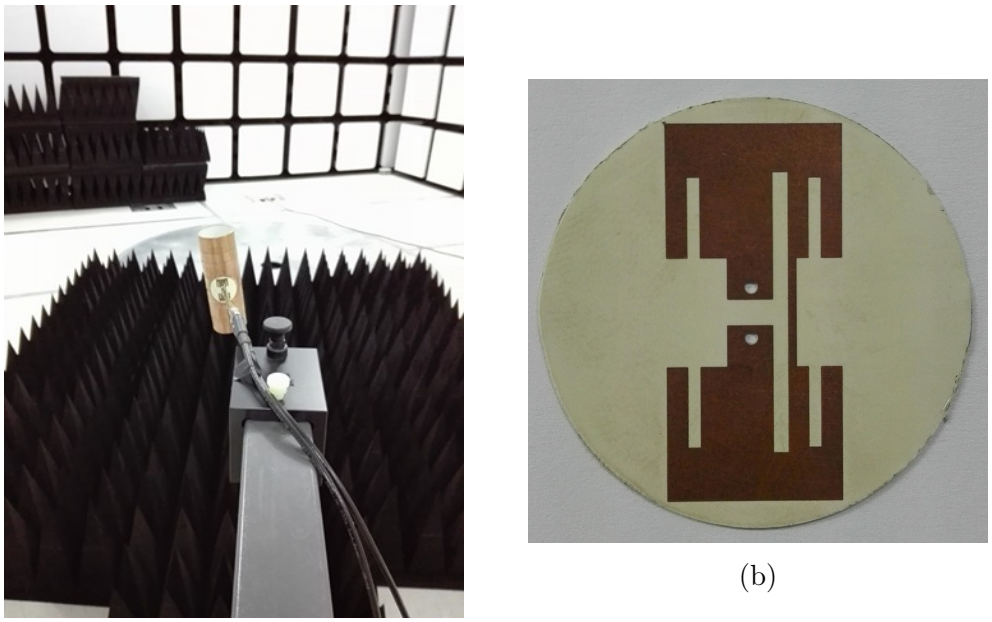

(a) (b)

Figure 4.5: a) Measurement developed in anechoic chamber, (b) prototype built.

4.4. Measurement results

Figure **4.6** shows the best measurement for reflection coefficient of the tag antenna. The central frequency of the tag antenna has a displacement of about 115 MHz in comparison to the expected results, obtained in the simulations. Therefore, the tag antenna is not tuned at

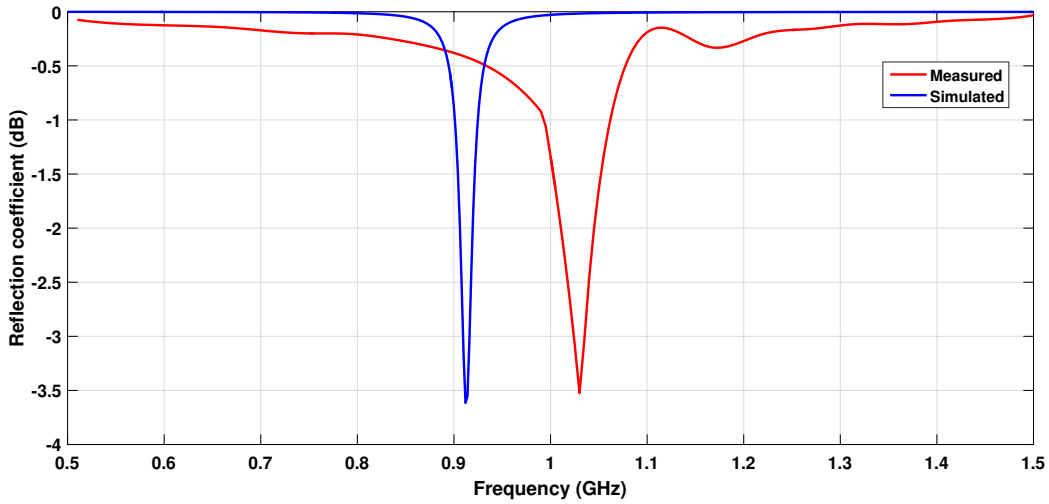

Figure 4.6: Measured and simulated reflection coefficient of the tag antenna.

the desired frequency.

Thus, the following section presents the possible effects which did not allow a proper antenna performance. Also, simulations in another software were developed to compare the results obtained of the optimized antenna. Thus, using CST Studio was not found discrepancy in the results regarding to HFSS. Furthermore, were developed new measurements using a feeding procedure through back side of antenna, to avoid the presence of the metallic structure in the direction of propagation. In this test was not seen any difference in regard to the previous results.

4.5. Possible effects that prevented the proper antenna performance

In this section, the possible factors and effects generated by the manufacturing process of the tag antenna are analyzed, which prevented the proper results in the measurements process with respect to the simulations. The effects are analyzed independently, as follows:

a) The incorrect position of the feeding points in the dipole antenna. After the antenna was built, it was seen that the feeding points were not located on the dipole's edges. Thus, the parameter b of the tag antenna changed its value from 2 mm to 4 mm, generating that the current density distribution on the dipole, in the real scenario, may be different than the obtained in the simulations. Also, this issue generates that the resonance frequency

of the antenna increases 14 MHz on the expected value, as shown in Figure **4.7**, where is depicted the reactance curves for three different values of parameter b.

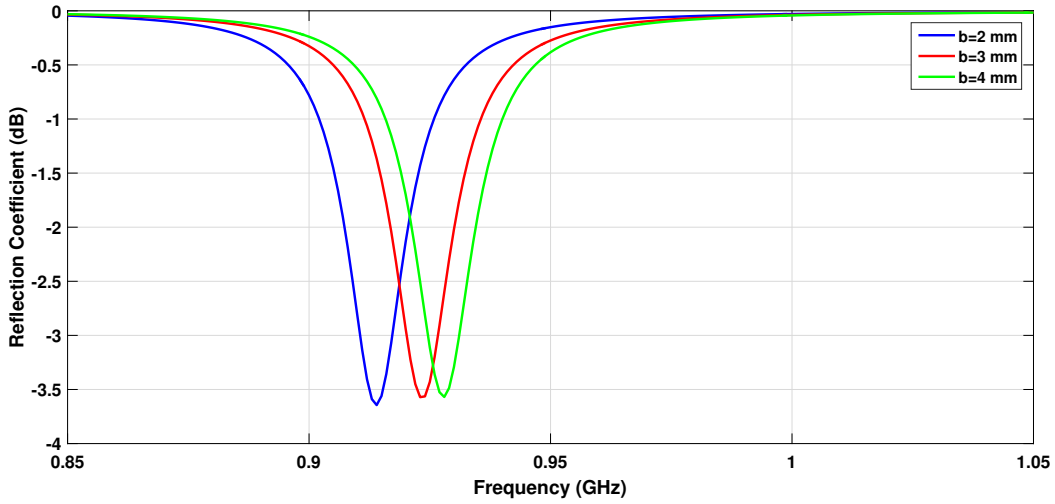

Figure 4.7: Reflection coefficient of the antenna for a variation of the parameter b.

b) Material for antenna design. As was mentioned in this work, the antenna was modeled as a PEC. However, for building effects, the antenna is manufactured with copper. Then, a simulation was done for knowing how the material can affect the resonance frequency of the tag antenna. Figure **4.8** illustrates the reflection coefficient of the tag antenna using a PEC and copper material. It is possible to observe that there is an displacement of 15 MHz between them.

c) Surface roughness effects and uncertainty in the electrical properties of the adhesive film. When a wave is propagated from free space ($\epsilon_r = 1$) to a different medium ($\epsilon_r > 1$), the wave propagation velocity tends to decrease (speed<speed of light). Thus, the roughness has an effect on the wave propagation constant and on the velocity [47], as illustrated in Figure **4.9**. For rough surfaces there is a slower propagation wave velocity. Therefore, the effective dielectric constant of the substrate is higher [48, 49]. The wave velocity (V_r)in the direction of wave travel can be expressed as:

$$V_r = \frac{1}{\sqrt{(\mu\epsilon)}} \tag{4.11}$$

Based on the information provided by Rogers Corporation, the substrate ULTRALAM 3850HT has a double copper clad laminate. Moreover, there are two different kinds of copper laminates. The first is the rolled-annealed (RA) foil, which is destined for planar circuit

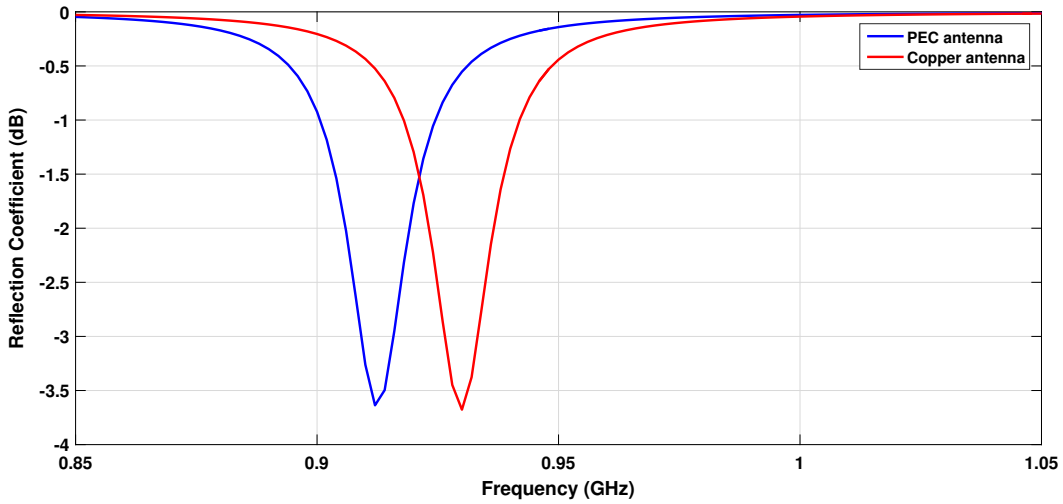

Figure 4.8: Reflection coefficient of the antenna modeled as PEC and copper.

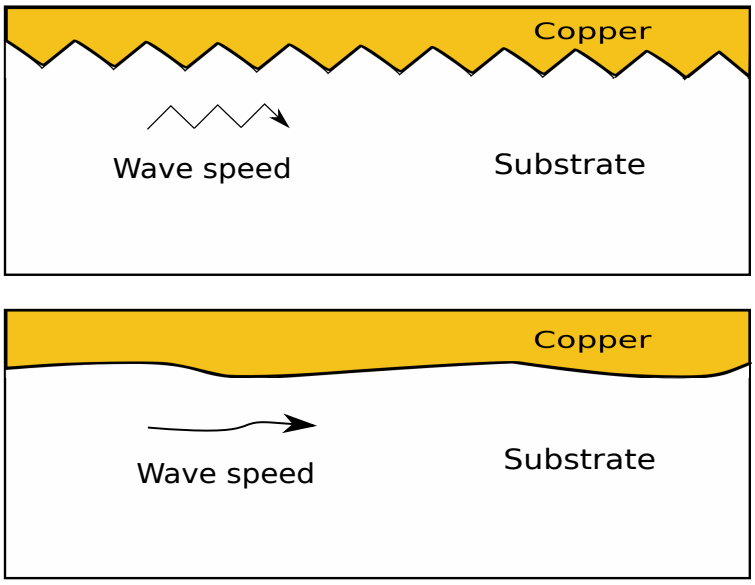

Figure 4.9: Propagation velocity wave on different surfaces

applications, and it contains a roughness of 0.3 μm RMS. The second type is the Electro-deposited (ED) foil, composed by plating from a copper sulfate bath and introduces a high roughness with a value of 1.8 μm RMS.

Furthermore, according with the fabrication process, a thin substrate has a higher roughness in the copper clad than a thicker substrate [50, 51]. Thereby, the roughness has an influence on the effective dielectric constant and the dielectric loss of the substrate. In the literature exists some methods to compute the insertion loss in function of the roughness. The model

proposed by Hammerstad and Jensen [48, 50], incorporates a multiplicative correction factor (K_{SR}), which it is very important to calculate the wave attenuation constant and the insertion loss, as follows:

$$\alpha_{cond,rough} = \alpha_{cond,smooth} * K_{SR} \tag{4.12}$$

Where $\alpha_{cond,smooth}$ is the attenuation constant calculated for a smooth conductor.

$$K_{SR} = 1 + \frac{2}{\pi} \tan^{-1} \left(1.4 \left[\frac{R_{RMS}}{\delta} \right]^2 \right) \tag{4.13}$$

Where R_{RMS} is the RMS value of roughness in the conductor layer of the substrate and δ is the skin depth. Hence, based on the last equation, when the copper roughness is high, the value of K_{RMS} is large too. Therefore, the attenuation constant and the insertion loss increase in regard to smooth conductor.

On the other hand, the electromagnetic principle of microstrip antennas is used to obtain an approximation of the effective dielectric constant of the substrate, considering the fringing effects in antennas. The following equation allows to compute the effective dielectric constant, for W/h >1, without considering roughness effects.

$$\epsilon_{eff} = \frac{\epsilon_r + 1}{2} + \frac{\epsilon_r - 1}{2} \left[1 + 12 \left(\frac{h}{W} \right) \right]^{-1/2} \tag{4.14}$$

Where ϵ_r is the relative permittivity of the substrate, W is the width of the antenna and h is the substrate thickness.

The amount of fringing is a function of the dimensions of the patch and the height of the substrate. As $W/h \gg 1$, the electric field lines concentrate mostly in the substrate, making the microstrip line seems wider electrically [21]. Thus, the effective dielectric constant is closer to the intrinsic permittivity of the substrate (also named Process DK=2.9).

Nevertheless, considering the effect produced by roughness on the electrical parameters of the substrate, a new complex permittivity is modeled.
The relative complex permittivity of a dielectric can be expressed as follows:

$$\dot{\epsilon}_r(\omega) = \frac{\dot{\epsilon}(\omega)}{\epsilon(\omega)} = \epsilon'(\omega) - j\epsilon''(\omega) \tag{4.15}$$

where ϵ' and ϵ'' are the real and imaginary part of the relative complex permittivity of the

material, which depend on the frequency. Also, ϵ'' represents the electric losses of the material due to its dielectric characteristics, tending to increase with an increment in the frequency [33]. Consequently, appears a new term which specifically define the electric loss tangent (δ), as expressed in the following equation.

$$\tan\delta = \frac{\epsilon''}{\epsilon'} \tag{4.16}$$

Based on the roughness effects analyzed in this section, equation (4.15) can be modified including a new term (ΔR) which models the roughness in the copper layer of the substrate, as shown in equation (4.17), in order to compute its effective dielectric constant.

$$\dot{\epsilon}_r(\omega) = [\epsilon'(\omega) + \epsilon'(\Delta R)] - j\,[\epsilon''(\omega) + \epsilon''(\Delta R)] \tag{4.17}$$

On the other hand, Rogers Corporation provides two dielectric constants, based on two different test. The first test, named microstrip differential phase-length method, provides a permittivity named "Design DK" with a value of 3.14. It is a transmission/reflection method based on two transmission-line circuits as guidelines with different physical lengths. Moreover, the Design Dk of the substrate 3850HT is computed by one laminate of the selected material with thickness 0.01 mm and a roughness in the ED copper clad of $1.8\mu m$ RMS[52, 53].

The second method is denominated clamped stripline resonator test. It is used for standard Quality Assurance (QA) testing of the permittivity "Process Dk", which it is a second dielectric constant provided by Rogers Corporation in the substrate data sheet with a value of 2.9 [54]. This method is widely adopted by the industry because it is repeatable, accurate, fast and evaluates the intrinsic permittivity of the substrate.

In this way, the Design DK is not appropriated for this work, because the measurement conditions and application of this test are not compatible for the selected scenario in this research, due to in this work is used a substrate with a higher thickness. Thus, it is necessary to consider an intrinsic permittivity of the substrate, which provides the proper electrical properties.

Microwave Impedance Calculator (MIC) is a software provided by Rogers Corporation which analyzes the electrical parameters of substrates, considering the fringing and roughness effects. Then, according to the information provided for the software, the substrate permittivity is around of 2.9 and its dielectric loss is 0.0078, for a single substrate ULTRALAM 3850HT with thickness of 0.35 mm. The loss tangent was higher as consequence of the insertion of roughness effect on the electrical parameters of the substrate. Thus, the relative complex permittivity of the substrate can be expressed as:

$$\begin{aligned} \epsilon_{eff} &= 2.9 \\ \tan\delta &= 0.0078 \end{aligned} \tag{4.18}$$

Figure **4.10** illustrates the behavior of the tag antenna considering the electrical parameters of the substrate with the roughness effect (DK=2.9 and DF=0.0078) in comparison with the initial conditions (without roughness effect, DK=3.14 and DF=0.002) used in the antenna optimization. Here, there is a displacement in the operating frequency of 36 MHz between the two mentioned scenarios.

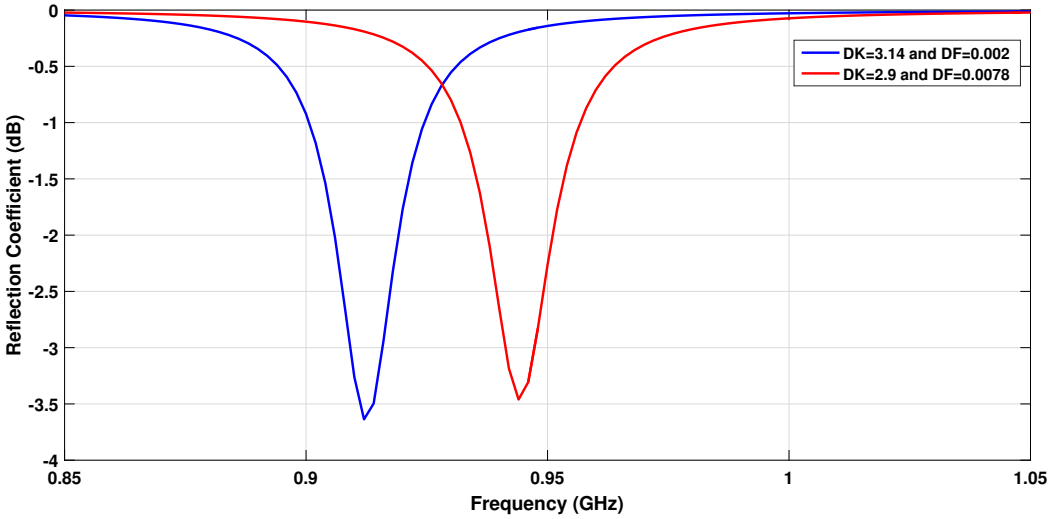

Figure 4.10: Reflection coefficient of the antenna for a variation in the electrical properties of the substrate.

4.6. Comparison between measurements vs simulations

In this section, a graphic comparison between the measurements and simulations of the tag antenna is depicted. This is performed with the aim to justify the possible effects that prevented the proper antenna performance. Therefore, Figure **4.11** illustrates the reflection coefficient of the tag antenna when it is attached on a copper cylinder with radius=20 mm, for three specific cases: measured result, simulation based on the optimized antenna without to consider any limitation, and simulation considering the non-modeled effects. For these cases, the substrate was modeled as a single dielectric with thickness of 0.4 mm (including the adhesive film).

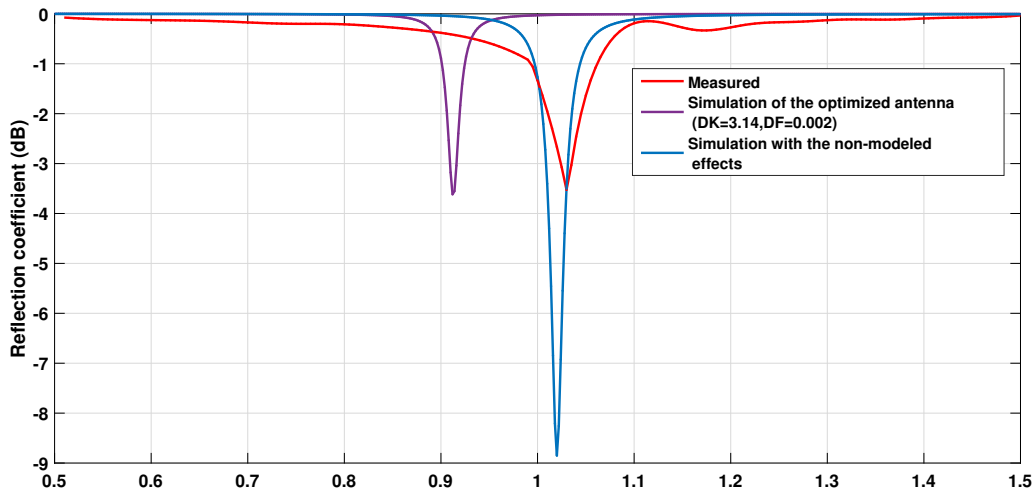

Figure 4.11: Comparison measurements vs simulations for reflection coefficient of the tag antenna attached on copper cylinder with radius=20 mm.

The effective dielectric constant for a single substrate of 0.4 mm was calibrated by simulations, in order to obtain a similar performance with respect to the measurements, as shown in Figure **4.11**. Therefore, a DK=2.6 and DF=0.03 were achieved, allowing to affirm that the adhesive film has dielectric properties which affects the dielectric characteristics of the substrate. Then, the dielectric loss tangent of the substrate, including the adhesive film, is approximately ten times the dielectric loss of the ULTRALAM 3850 HT laminate.

The adding of the adhesive film, which does not have a uniform physical characteristic, can include air sections inside the dielectric layer, which introduce a low permittivity and a high loss tangent. Then, its electrical parameters were calibrated by simulations, obtaining a dielectric constant of about 1.6 and a dielectric loss tangent of 0.08 for reaching the antenna tuning at measured operating frequency.

4.7. New prototype with corrected issues

In this section, a new prototype was designed using the optimization tool. The design was based on the correction of previous issues which prevented the proper antenna performance at desired frequency band. Here, the adhesive film was not used. However, a thin layer of air was considered in the middle of two dielectrics with a thickness of 21 μm (equivalent around of six times the roughness thickness), which produces that the effective dielectric constant of the substrate is equal to 2.6.

Table **4.1** shows the parameters of the optimized antenna mounted on copper cylinder with radius=20 mm, using genetic algorithm.

Table 4.1: Parameters and dimension of the corrected tag antenna mounted on a copper cylinder using genetic algorithm.

Parameter	**Length (mm)**	**Parameter**	**Length (mm)**	**Parameter**	**Length (mm)**
a	3.35	f	8.2	n	0.9
b	2	g	6	o	9.9
c	1.2	h	0.35	p	21
d	2	i	1	L	28
e	0.55	m	1.5	W	13

Figure **4.12** illustrates the measured reflection coefficient of the tag antenna, based on the developed corrections for the new prototype. The antenna is tuned in the 902-928 MHz frequency band with a reflection coefficient of -6.8 dB, showing a proper behavior regarding to the simulations.

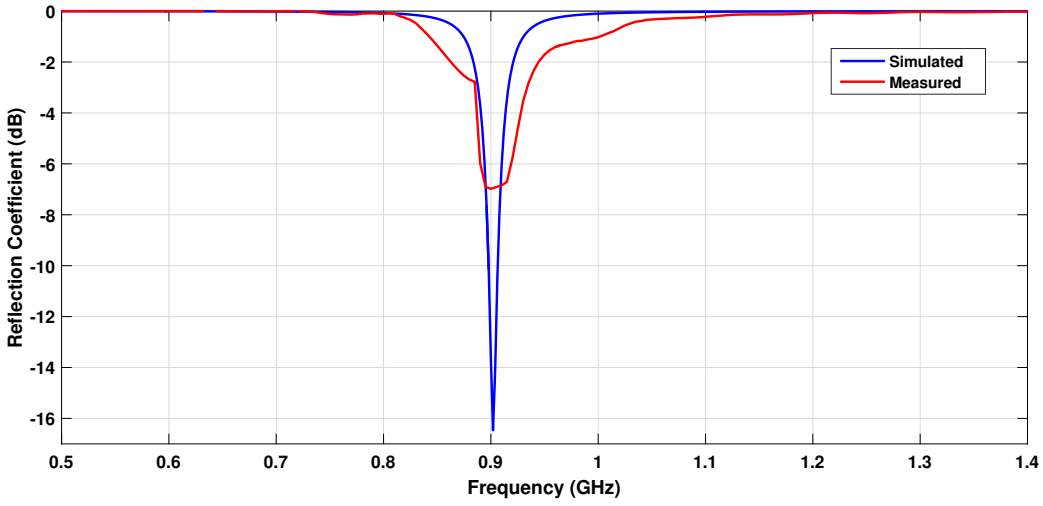

Figure 4.12: Measured and simulated reflection coefficient of the corrected tag antenna.

Finally, Figure **4.13** shows the read range of the tag antenna based on the simulations. The read range of the new prototype is about of one meter in the desired frequency band, which

it is a proper coverage for RFID applications over cylindrical metallic surfaces.

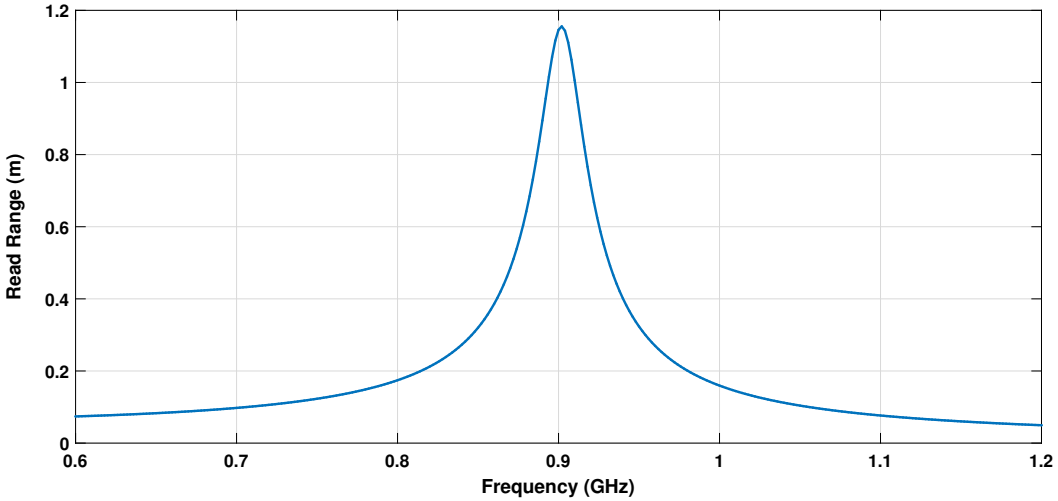

Figure 4.13: Simulated read range of the corrected tag antenna.

5 Conclusions and future works

5.1. Conclusions

The proposed small and flexible RFID tag antenna which operates at UHF frequency band of 915 MHz can be wrapped on cylindrical metallic surfaces with read ranges above one meter. The best results are obtained for a high antenna curvature, due the increase of the radiation efficiency and gain of the tag antenna, which improve its performance.

The tag antenna is considered unsuitable to work on flat objects since the read range is low. This limitation is produced due to the low radiation efficiency and low antenna gain, that limit the good performance of the tag.

The proposed RFID tag antenna can be wrapped on cylinder surfaces fabricated with polyethylene terephthalate (PET) materials. The results show that the dipole antenna can operate using a commercial substrate with flexible characteristics in a read range about one meter.

When it is added a liquid content inside the PET material is generated a multilayer dielectric which increases the effective permittivity. Also, the existence of ground plane helps to create an independence between the liquid permittivity and the resonance frequency of the antenna, which allows to maximize the read range of the tag antenna in the desired operating frequency.

The low substrate thickness and the roughness effect in the copper clad affect the effective dielectric constant and dielectric loss tangent of the substrate. Moreover, the adhesive film adds a low permittivity and a high dielectric loss tangent in the substrate, producing an displacement of the resonance frequency. Therefore, the roughness effect and the dielectric properties of the adhesive film must be considered in the small antenna design.

The roughness in the substrate is the most significant effect among the analyzed problems. This effect modifies the electrical performance of small and slim antennas. Specifically, the complex effective dielectric constant and resonance frequency are electrical parameters very sensitive to the substrate thickness due to the roughness in the double copper clad laminate.

5.2. Future works

Characterizing and studying more deeply the electrical properties of the substrate including the adhesive film. Another possibility is the use of the adhesive film ULTRALAM 3908 suggested by Rogers Corporation to attach the two substrate laminates. Then, it is possible to avoid the uncertainly of the effect which this layer can creates on the effective dielectric constant of the substrate.

Developing measurements of the tag read range with a commercial reader in an environment free of electromagnetic noise using the anechoic chamber, and inside a real scenario where may be used the tag.

Researching other methods to conjugate the impedance matching and to study the viability of the implementation of meta-materials structures on the ground plane to improve the antenna performance.

Performing an analysis of electromagnetic interference produced for elements surrounding to the tag antenna, studying how the reflecting and refracting events can damage the radiation pattern of the tag antenna, and how is affected the antenna performance with the presence of a second energy source.

Analyzing the viability of implementation of chipless technology on the proposed antenna, to avoid the impedance matching problems, defining a size/performance ratio in the antenna to maintain its applicability on small curved metallic surfaces.

Developing a deeper analysis of the antenna curvature on the tag performance, evaluating the different TM modes that affect the resonance frequency and the radiation field solution through of implementation of an analytic formulation.

Optimizing and design a new small antenna with a broad bandwidth characteristics to tune the antenna in the desired frequency and to avoid the abrupt variations of read range of the tag in its overall bandwidth.

References

[1] K. V. S. Rao, S. Member, P. V. Nikitin, and S. F. Lam, "Antenna Design for UHF RFID Tags : A Review and a Practical Application," vol. 53, no. 12, 2005.

[2] A. Babar, P. Kallio, and L. Ukkonen, "Small and Flexible Metal Mountable Passive UHF RFID Tag on High-Dielectric Polymer-Ceramic Composite Substrate," *IEEE antennas and wireless propagation letters*, vol. 11, pp. 1319–1322, 2012.

[3] H. Stockman, "Communication by Means of Reflected Power," *Proceedings of the IRE*, vol. 36, no. 10, pp. 1196–1204, 1948.

[4] EPoSS, *Internet of Things in 2020: A Roadmap for the future*. 2008.

[5] S. Li, L. D. Xu, and S. Zhao, "The internet of things: a survey," *Information Systems Frontiers*, vol. 17, no. 2, pp. 243–259, 2015.

[6] A. A. Babar, V. A. Bhagavati, L. Ukkonen, A. Z. Elsherbeni, P. Kallio, and L. Syd, "Performance of High-Permittivity Ceramic-Polymer Composite as a Substrate for UHF RFID Tag Antennas," *Internation Journal of Antennas and Propagation*, vol. 2012, 2012.

[7] S. Sajal, Y. Atanasov, B. D. Braaten, V. Marinov, and O. Swenson, "A low cost flexible passive UHF RFID tag for sensing moisture based on antenna polarization," *IEEE International Conference on Electro Information Technology*, pp. 542–545, 2014.

[8] A.-i. Petrariu and V. Popa, "Low Profile Flexible Metal Mountable UHF RFID Tag Antenna," vol. 2, no. 1, 2015.

[9] S. Dey, N. Saha, and A. Alomainy, "Design and performance analysis of narrow band textile antenna for three different substrate permittivity materials and bending consequence," *LAPC 2011 - 2011 Loughborough Antennas and Propagation Conference*, pp. 2–6, 2011.

[10] H. A. Wheelert, "Fundamental Limitations of Small Antennas," pp. 1479–1484, 1947.

[11] J. Volakis, K. Fujimoto, and C. Chen, *Small Antennas:Miniaturization Techniques and Applications*. 2010.

[12] D. Kim, J. Yeo, and A. Abstract, "Low-Profile RFID Tag Antenna Using Compact AMC Substrate for Metallic Objects," *IEEE antennas and wireless propagation letters*, vol. 7, pp. 2008–2010, 2009.

[13] H. Rajagopalan and Y. Rahmat-samii, "Platform Tolerant and Conformal RFID Tag Antenna : Design , Construction and Measurements," vol. 25, no. 6, pp. 486–497, 2010.

[14] N. M. Faudzi, M. T. Ali, I. Ismail, H. Jumaat, and N. H. M. Sukaimi, "Compact Microstrip Patch UHF-RFID Tag Antenna For Metal Object," pp. 160–164, 2014.

[15] C. M. Krowne, "Cylindrical-Rectangular Microstrip Antenna," *IEEE Transactions on Antennas and Propagation*, vol. 31, no. 1, pp. 194–199, 1983.

[16] K.-M. Luk, K.-F. Lee, and J. Dahele, "Analysis of the Cylindrical-Rectangular Patch Antenna," *IEEE Transactions on Antennas and Propagation*, 1989.

[17] "Compact metal mountable UHF RFID tag on a barium titanate based substrate," *Progress In Electromagnetics Research C*, vol. 26, no. November 2011, pp. 43–57, 2012.

[18] NXP Semiconductor, "SL3S1203_1213 UCODE G2iL and G2iL+ IC Chip," no. 32, 2014.

[19] M. Bolic and I. Stojmenovic, *RFID systems Research Trends and Challenge*. first edition, 2010.

[20] Rogers Corporation, "Datasheet Ultralam ® 3850ht," pp. 1–2.

[21] C. Balanis, *Antenna Theory: Analysis and Design*. No. 3, 3th ed., 2005.

[22] Rogers Corporation, "Datasheet ULTRALAM ® 3908 Bondply /ULTRALAM 3000 Series," pp. 1–2.

[23] T. Björninen, A. Elsherbeni, and L. Ukkonen, "Performance of Single and Double T-matched Short Dipole Tag Antennas for UHF RFID Systems," *Applied Computational Electromagnetics Society Journal*, no. December, 2011.

[24] G. Marrocco, "The Art of UHF RFID Antenna Design : Impedance-Matching and Size-Reduction Techniques," *IEEE Antennas and Propagation Magazine*, vol. 50, no. 1, 2008.

[25] J. Choo, J. Ryoo, J. Hong, H. Jeon, C. Choi, and M. M. Tentzeris, "T-matching Networks for the Efficient Matching of Practical RFID Tags," no. October, pp. 5–8, 2009.

[26] A. Babar and L. Ukkomen, "RFID Tags for challenging environments," *IEEE microwave magazine*, no. August, pp. 2–7, 2013.

[27] H. Ahmed, N. Muqarrab, M. R. Zaffar, J. U. R. Kazim, and I. Irfanullah, "A compact passive UHF RFID meandered dipole tag," *Proceedings of the 2016 19th International Multi-Topic Conference, INMIC 2016*, pp. 9–12, 2017.

[28] N. A. Mohammed, *Analysis and Synthesis of UHF RFID Antennas using the Embedded T-match*. PhD thesis, Universisty of Kansas, 2010.

[29] Á. P. d. M. Fernández and R. Jesús, "Algoritmo del elipsoide interior para programación lineal," *Qüestiió*, vol. 15, no. June, pp. 69–93, 1991.

[30] O. Botero and H. Chaouchi, "RFID network topology design based on Genetic Algorithms," *2011 IEEE International Conference on RFID-Technologies and Applications*, vol. 2011, pp. 300–305, 2011.

[31] G. Marrocco, "Gain-Optimized Self-Resonant Meander Line," vol. 2, pp. 302–305, 2003.

[32] A. Elrashidi, K. Elleithy, and H. Bajwa, "Effect of Curvature on the Performance of a Microstrip Printed Antenna Conformed on Cylindrical Body Using Epsilam-10 Ceramic-Filled Teflon as a Substrate," no. November, 2011.

[33] C. Balanis, *Advanced engineering electromagnetics*. 2th ed., 2012.

[34] S.-l. Chen, "A Miniature RFID Tag Antenna Design for Metallic Objects Application," *IEEE antennas and wireless propagation letters*, vol. 8, no. c, pp. 1043–1045, 2009.

[35] T. Björninen, A. Z. Elsherbeni, and L. Ukkonen, "Low-profile conformal UHF RFID tag antenna for integration with water bottles," *IEEE Antennas and Wireless Propagation Letters*, vol. 10, pp. 1147–1150, 2011.

[36] M. Ryan and M. Frater, *Communications and information systems*. Canberra: Argos Press P/L, 2002.

[37] E. Da Silva, *High frequency and microwave engineering*. Oxford: Newnes, 2001.

[38] H. Kogure, J. Rautio, and Y. Kogure, *Introduction to antenna analysis using EM simulators*. Artech House, 2011.

[39] X. Qing, C. K. Goh, and Z. N. Chen, "Impedance characterization of rfid tag antennas and application in tag co-design," *IEEE Transactions on Microwave Theory and Techniques*, vol. 57, no. 5, pp. 1268–1274, 2009.

[40] K. D. Palmer and M. W. van Rooyen, "Simple broadband measurements of balanced loads using a network analyzer," *IEEE Transactions on Instrumentation and Measurement*, vol. 55, no. 1, pp. 266–272, 2006.

[41] T. Koskinen and Y. Rahmat-samii, "Metal-Mountable Microstrip RFID Tag Antenna for High Impedance Microchip," pp. 2791–2795.

[42] Rohde & Schwarz, "R & S ® ZVL Vector Network Analyzer Specifications," tech. rep., 2017.

[43] Rohde & Schwarz, "R & S ® ZV-Z170 Calibration Kit Specifications," 2012.

[44] JBM Instruments, "N-type JBM J2061 Calibration Kit Specifications," Tech. Rep. 35, 2009.

[45] M. Paixão and D. Oliveira, "Medição da Impedância de Entrada de Antenas RFID," tech. rep., Universidade Federal de Minas Gerais, 2014.

[46] X. Qing, C. K. Goh, and Z. N. Chen, "Impedance characterization of rfid tag antennas and application in tag co-design," *IEEE Transactions on Microwave Theory and Techniques*, vol. 57, no. 5, pp. 1268–1274, 2009.

[47] S. Kahraman, "The effects of fracture roughness on P-wave velocity," no. January, 2016.

[48] A. F. Horn, J. W. Reynolds, and J. C. Rautio, "Conductor profile effects on the propagation constant of microstrip transmission lines," *IEEE MTT-S International Microwave Symposium Digest*, pp. 868–871, 2010.

[49] X. Guo, D. R. Jackson, and J. Chen, "An analysis of copper surface roughness effects on signal propagation in PCB traces," *Texas Symp. on Wireless and Microw. Circuits Syst. (WMCS)*, 2013.

[50] J. Reynolds and P. LaFrace, "Effect of conductor profile on the insertion loss, phase constant, and dispersion in thin high frequency transmission lines," tech. rep., Rogers Corporation, 2010.

[51] Rogers Corporation, "What RF Circuit Designers need to know about Dk," 2015.

[52] R. Corporation, "Apparent dielectric constant of high-frequency PCBs," no. December, pp. 10–13, 2010.

[53] Rogers Corporation, "Common Test Methods for Measuring Dielectric Constant," 2014.

[54] Rogers Corporation, "Learn to Apply Design Dk - Rogers Corporation Blog," 2011.